

Review: Layer-Number Controllable Preparation of High-Quality Graphene for Wide Applications

Yun-Bin Xie^{1,2,3}, Mei-Rong Huang^{1,2} and Xin-Gui Li^{1,2*}

(1. State Key Laboratory of Pollution Control and Resource Reuse, and Shanghai Institute of Pollution Control and Ecological Security,

College of Environmental Science and Engineering, Tongji University, 1239 Siping Road, Shanghai 200092, China;

2. Key Laboratory of Advanced Civil Engineering Materials of Ministry of Education, College of Materials Science and Engineering,

Tongji University, 1239 Siping Road, Shanghai 200092, China;

3. Shanghai Weikai Optoelectronic New Materials Co., Ltd., 2055 Kunyang Road, Shanghai 201111, China)

Abstract: Graphene, a well-known two-dimensional (2D) material, has sparked broad enthusiasm in both scientific and industrial communities in these years, due to its exceptional electrical, thermal, mechanical, and versatile properties. However, many properties and applications of graphene are layer-number dependent. The preparation of high-quality graphene with controlled layer numbers is full of challenge, since it varies much with the synthesis routes and relevant experimental conditions. Hence, there is an urgent need to improve the layer-number controllability of graphene preparation. Generally, graphene can be prepared by two complementary approaches: “top-down” and “bottom-up”. Since they have their own advantages, the recent advances in the layer-number tunable preparation of high-quality graphene are separately studied from the two aspects in this review, especially those dedicated to single parameter. Some effective strategies are discussed in detail, mainly including 1) supercritical-CO₂ assisted sonication, electrochemical exfoliation of graphite intercalation compounds, and layer-by-layer thinning with plasma or laser, for “top-down” graphene; 2) chemical vapor deposition (CVD) on dual-metal substrate, ion-implantation CVD, layer-by-layer CVD, plasma-enhanced CVD, layered-double-hydroxides template-assisted CVD; and 3) graphite-enclosure assisted epitaxial growth and pulsed-magnetron-sputtering assisted physical vapor deposition for “bottom-up” graphene on various substrates. In addition, the respective advantages of graphene with different layer numbers in properties and applications are also presented. Finally, the contribution concludes with some important perspectives on the remained challenges and future perspectives.

Keywords: graphene, nanosheet preparation, controllable layer number, tunable morphology, high quality graphene

CLC number: O613; TB332

Document code:A

1 Introduction

In the past decade, graphene, an emerging two-dimensional (2D) material of sp^2 -bonded carbon honeycomb lattice, has become one of the most attractive topics in both research and industry sectors.

It has exhibited excellent electrical, mechanical, thermal, and many other fascinating properties that result in versatile application potentials [1-4]. For example, its unique electrical properties (adjustable electrical conductivity as high as $\sim 10^6 \text{ S} \cdot \text{m}^{-1}$) and

Received 2020-01-21.

Sponsored by the JSPS Invitational Fellowship for Research in Japan (Grant No. L18516) and the National Natural Science Foundation of China (Grant No. 51273148).

* Corresponding author. Distinguished Professor of CheungKong (ChangJiang) Scholars. Email: lixingui@tongji.edu.cn

super-low density (as low as $0.03 \text{ g}\cdot\text{cm}^{-3}$) have made it one of the most promising light-weight electroconductive materials, as compared with the traditional metal conductors and the well-known conductive polymers such as polyaniline and polypyrrole^[5-9].

However, most of the remarkable properties of graphene demonstrate strong layer-number

dependence^[2, 10]. Generally, compared with multiple-layer graphene, single-layer graphene (SLG) exhibits much better performance in electroconductivity, thermal conductivity, and transparency, as presented in Fig. 1(b)-(c). Nevertheless, some properties may reach the optimal value in few-layer graphene (FLG) rather than SLG, such as the Young's modulus (Fig. 1(a)) and self-lubricating property (Fig. 1(d)).

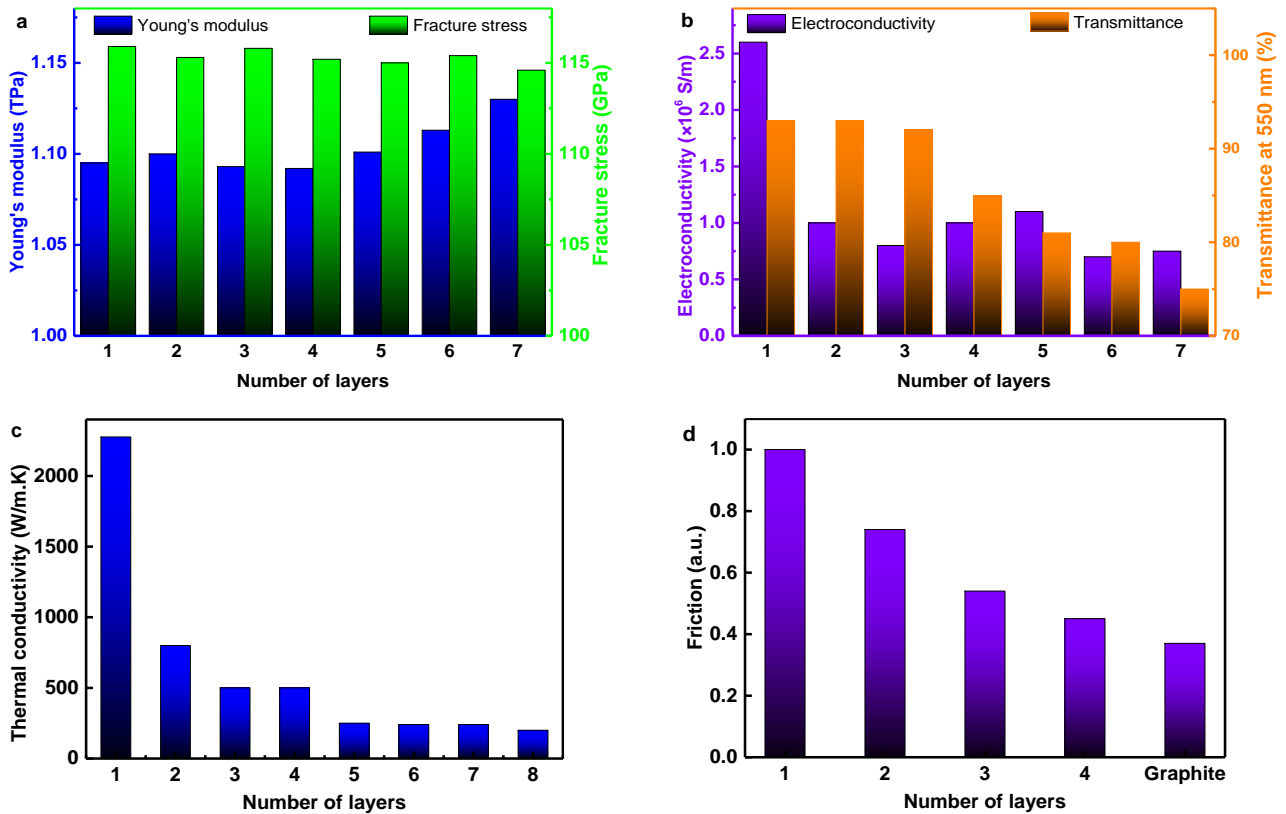


Fig. 1 Layer-dependent properties of graphene: (a) Young's modulus and fracture stress^[11] (b) Electroconductivity and transmittance at 550 nm^[12] (c) Thermal conductivity^[13] (d) Self-lubricating property characterized by friction^[14]

In addition, during the past years, more and more unique properties and application potentials have been found for graphene with few layers^[15]. For example, due to its zero energy band-gap structure, SLG suffers from a serious current leakage in electronic devices, whereas the Bernal-stacked BLG and Rhombohedral-stacked three-layer graphene (TLG) have been found to perfectly solve the problem owing to opened bandgaps^[16-18]. Besides, it is believed that TLG and

four-layer graphene are more attractive in many applications, especially electronic and optical devices^[19-20]. In addition, tunable optical and electrical properties can be easily achieved by FLG^[21-22].

Hence, it is of great significance to synthesize graphene with different layer numbers – not only SLG, but also BLG, TLG, and FLG^[23-24]. Particularly, it would be quite exciting if graphene with controlled

layers could be prepared through the simple adjustment of certain parameter based on one method.

In general, graphene can be prepared by two classes of methods^[25-26]: 1) The “top-down” approach, e.g., liquid-phase exfoliation which usually provides graphene in the forms of powder or dispersion, has great advantages in scalability and cost-efficiency as well as a very wide range of applications such as conducting additives in various composites^[27-29]; 2) The “bottom-up” approach, usually referring to chemical vapor deposition (CVD) of hydrocarbons on metal substrates (e.g., nickel) and epitaxial growth on SiC, aims to prepare large-area and high-quality graphene that could be used in the future microelectronics industry^[30-31]. Actually, these are two complementary strategies. For example, the production of transparent electrodes and sensors require large-area graphene, whereas graphene-based nanocomposites and energy storage devices ask more for bulk quantities of graphene^[20].

However, both of them meet great challenge to synthesize high-quality graphene with desired layer numbers, due to their respective limitations^[32-34]. For instance, the CVD growth of graphene is influenced by many factors such as the substrates, the carbon sources, and complicated process conditions, which brings about much uncertainty to the layer numbers and the thickness uniformity of the obtained graphene^[33-34].

Many efforts have been devoted to the controllable synthesis of graphene in the past several years, including the strategies for the preparation of graphene with controlled morphology or doping levels^[35-36]. However, no systematical review focused on the layer-number controllability of high-quality graphene has been found so far. For an overall understanding and further promotion of the controllable preparation of graphene, here the recent progress on the layer-number controllable preparation of graphene is reviewed based on the above two

methods, focusing on the synthesis strategy for high-quality pristine graphene. In this work, the quality of graphene is largely assessed by two indexes: 1) lateral size, which is usually characterized by TEM or AFM and expected to be greater than a few micrometers; 2) defects level, indicated by the intensity ratio of the Raman D (I_D) and G (I_G) peaks (I_D/I_G), where a smaller I_D/I_G value suggests a lower defects level. In the same way, the layer numbers or thickness of graphene can be judged from the intensity ratios of I_{2D}/I_G , where a higher I_{2D}/I_G value corresponds to thinner graphene-layer^[37-38]. Obviously, for high-quality graphene, both a larger lateral size and lower defects level are preferred^[20].

2 Layer-Number Controllable Preparation of “Top-Down” Graphene

Here, the “top-down” graphene refers to the graphene exfoliated from graphite by top-down methods such as liquid-phase exfoliation. The biggest advantage of “top-down” graphene over “bottom-up” graphene lies in that it can be deposited on different substrates and used in a variety of environments^[26]. Especially, it can be employed to produce graphene-based composites or films, which greatly broaden the application of pristine graphene. Besides, top-down methods usually exhibit greater potentials in scalable production of graphene in large quantity. Therefore, studies on the controllable synthesis of top-down graphene are not only necessary but also of great significance.

2.1 Liquid-Phase Exfoliation

Liquid-phase exfoliation refers to the exfoliation of graphite in liquid media such as some proper solvents (e.g., *N*-methyl-2-pyrrolidone) or surfactants (e.g., sodium dodecyl sulfate). It is well-recognized as a

versatile and scalable method to produce graphene nanosheets (GNS). GNS can be extensively employed to produce composites for various applications, such as thin-film transistors, conductive transparent electrodes, light-emitting diodes, and photovoltaics^[39-44]. However, there are so many factors that influence the exfoliation and stability of the GNS, such as the type of the starting graphite and the liquid media, as well as the energy density and duration of sonication^[22, 45-47]. Thus, it is of great challenge to prepare high-quality GNS with controlled layer numbers by this method, and only a few studies can be found^[22, 48-49].

Wang et al.^[50] reported the successful synthesis of layer-number controllable GNS using ultrasound in supercritical CO₂, which can easily diffuse between the graphene layers due to its high diffusivity, low viscosity, and small molecule size^[49, 51]. It has been demonstrated that the electrical conductivity of FLG exfoliated by shear-assisted supercritical CO₂ can reach a high level of 4.7×10^6 S/m^[52]. Ultrasonication can further weaken the van der Waals interactions

between the graphene layers and urgent need thus effectively exfoliate the graphite into thin GNS. It is well-recognized that the efficiency of exfoliation is greatly influenced by the power of ultrasonication. In virtue of the coupled effects of supercritical CO₂ and ultrasonication, they successfully prepared SLG, BLG, and FLG through 30 min-ultrasonication with preset ultrasonic power of 300 W, 120 W, and 60 W, respectively (Fig. 2). That is to say, in the highly-diffusive environment, the layer numbers of GNS can be controlled by the ultrasonic power. In addition, LiFePO₄/graphene composite cathode made from the as-exfoliated GNS exhibited remarkable electrochemical performance. The specific capacity was reported to be 160 mAh/g which is 94.7% of the theoretical capacity. The problem lies in that the lateral size of the obtained SLG (50 - 100 nm) turned to be quite small due to the enlarged ultrasonic power. Nevertheless, it really demonstrates the advantages of supercritical CO₂ in the controllable preparation of graphene with desired layer numbers.

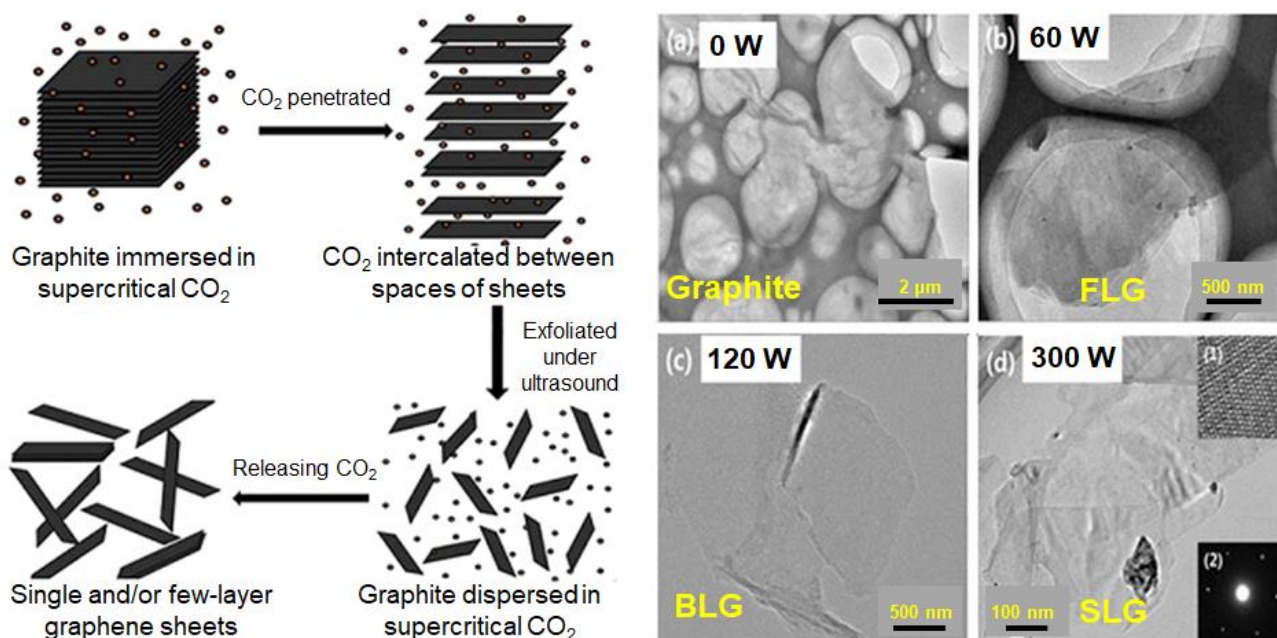


Fig. 2 (Left) Schematic illustration for the liquid-phase exfoliation of graphene by ultrasonic exfoliation in supercritical CO₂ (Right) TEM images of the exfoliated graphene under different ultrasound power: (a) 0 W; (b) 60 W; (c) 120 W; (d) 300 W, with inset HRTEM (1) and electron diffraction images (2)^[50]

It should be noted that the liquid-phase exfoliated

GNS usually turns out to be a mixture that consists

mainly of FLG and only a small fraction of SLG^[20]. To improve the productivity of SLG, Kovtyukhova et al.^[53-54] introduced a self-made Brønsted acid-intercalated graphite compounds as the starting material. The compounds were a mixture of graphite and 85 wt% H₃PO₄ that was coated on glass slides and kept at 120 °C for enough intercalation which could reduce the interlayer cohesive energy and facilitate the exfoliation to monolayers^[54]. After a systematic study on the medium polarity protic solvents such as isopropanol and *n*-pentanol, together with the temperature and the duration of the exfoliation process, they successfully obtained a yield of almost 100% SLG. Meanwhile, thanks to the gentle enough exfoliation process that would not disrupt the sp² π -conjugated system of graphene and preserve the crystalline integrity of graphene, the lateral size of the obtained SLG was as large as tens of microns. Although the preparation period of at least 2 days seems too long, it opens another door for the preparation of graphene with high yield of SLG together with good quality.

2.2 Electrochemical Method

Electrochemical exfoliation is a relatively simple, economic, and environment-friendly method. However, it had been less explored to prepare graphene nanosheets, due to the relatively numerous defects produced during the electrochemical process^[32, 55]. Only till the past few years, it received increasing attention as a potential scalable method for the preparation of graphene^[56].

To decrease the defects of graphene, Alanyalıoğlu et al.^[55] chose SDS solution as the electrolyte in the electrochemical exfoliation graphite, which could adsorb on the surface of graphene sheets and therefore prevent them from re-stacking. It was pointed out that the exfoliation could be ascribed to the horizontal intercalation of dodecyl sulfate anion (electrolyzed from SDS) into the basal plane of graphite. The

mobility and concentration of these anions could be tuned by the electrode potential. Thus, the layer numbers of graphene could be adjusted by the potential value for SDS intercalation into graphite. When the applied potential increased from 1.4V to 2.0V, the intensity ratio of the Raman 2D-band to G-band (I_{2D}/I_G) increased rapidly from ~0.15 to 0.31, which implied an obvious decline of the graphene thickness. According to the TEM results, the average size and thickness of the GNS prepared at 2.0 V were around 0.5 μ m and 1 nm, respectively, indicating that SLG could be achieved under a high potential value for intercalation. In addition, the final I_D/I_G ratio was found to be 0.12 which was quite close to that of the raw graphite (0.006), implying a low level of defects. Moreover, the obtained graphene/SDS suspension exhibited quite good stability for 8 months with no precipitation observed. However, it is a pity that the obtained graphene was a mixture of FLG and few SLG even after centrifuge, rather than graphene of certain layer(s) with narrow distribution.

For a better control of the graphene layer numbers, Wang et al.^[32] introduced another strategy named lithium conversion electrochemical reaction, based on a series of graphite intercalation compounds (GICs) which could be easily synthesized on a large scale. Firstly, CuCl₂-FeCl₃-GICs with different stage numbers were prepared by the insertion of CuCl₂-FeCl₃ layer between the graphite layers through a melt-salt method, which involved the calcination of the mixture of anhydrous FeCl₃, anhydrous CuCl₂, and natural graphite in a sealed reactor at 550-600 °C for 12 h. By adjusting the content of the reactants and the conditions of heat treatment, GICs with different stage numbers of 2, 4, and 6 were achieved. Then, the GICs were introduced as working electrode for electrochemical exfoliation (Fig. 3(a)). After an initial discharge/charge process, the compounds converted to a sandwiched composite in which the CuCl₂/FeCl₃/Fe/Cu layer was inserted between

graphene layers. Since the van der Waals forces of adjacent graphene sheets were destroyed, individual graphene layers could be simply exfoliated solely by a mild sonication. Accordingly, the graphene nanosheets with 2, 4, and 6 layers were successfully prepared by utilizing the GIC with stage number of 2, 4, and 6, respectively. In addition, the obtained BLG had a large lateral size of $\sim 8\ \mu\text{m}$ from the TEM image,

and exhibited a high electron mobility of about $4000\ \text{cm}^2\ \text{V}^{-1}\ \text{s}^{-1}$ at room temperature. Notably, no oxygen functional groups or defects were produced during the whole process, as proved by the TEM, AFM, and Raman results in Fig. 3(b-e). Although SLG was not available, it opens up a new avenue for producing high-quality graphene in a large scale.

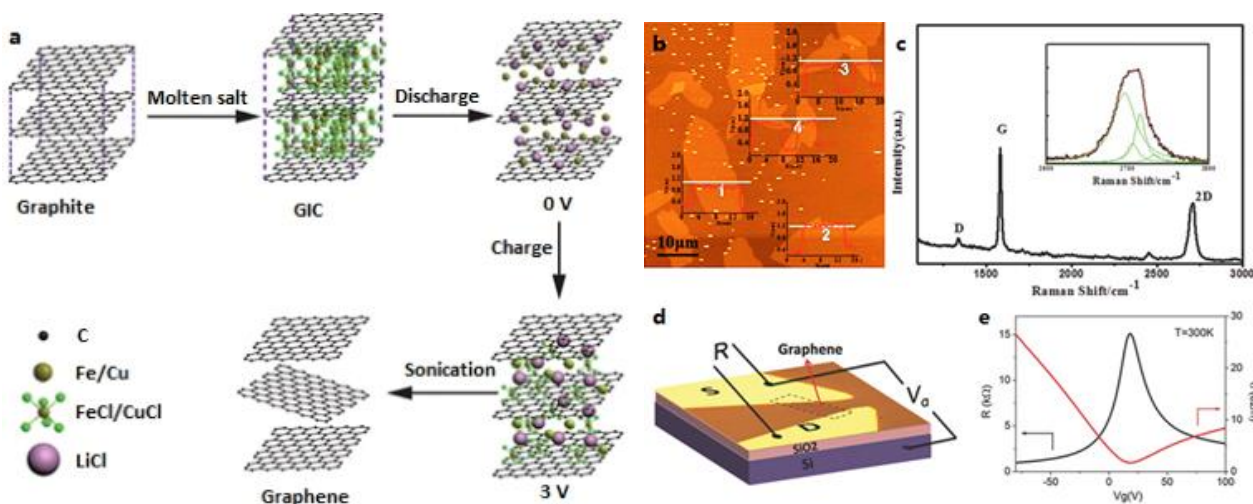


Fig. 3 (a) Scheme of electrochemical exfoliation of graphite intercalation compounds (GICs) for controllable preparation of graphene with different layer numbers (b) AFM image with height profile (c) Raman spectrum of the obtained BLG nanosheet (d,e) Electronic characteristics of the corresponding BLG-FET device: the cross-sectional diagram (S = source; D = drain) and electronic resistance and conductance vs. applied gate voltage (e)^[32]

2.3 Layer-by-Layer Thinning

In 2010, Huang et al.^[57] demonstrated that graphene can be peeled layer-by-layer using Joule heating from transmission electron microscopy (TEM). Although it was far away from practical device fabrication, this broke a novel path in reducing the thickness of graphene to achieve desired layer numbers by the use of proper energy such as plasma and laser treatment^[58-60].

2.3.1 Plasma thinning

Plasma etching technique is a quite effective tool in thinning layered materials, which utilizes the direct bombardment effect of precursor gases such as

nitrogen, argon, hydrogen, etc. under proper energy of plasma treatment^[58-59, 61]. The gases and plasma energy is quite important, otherwise the obtained graphene may be inhomogeneous or have too much defects^[59].

Zhang et al.^[61] demonstrated the successful plasma-thinning of graphene from multiple to single layers on a semiconducting substrate of SiO_2/Si at room temperature. They utilized medium input power (300-500 W) which is strong enough to etch graphene layers but less invasive, and chose hydrogen and argon (Ar) as the precursor gas. Owing to its heavy molecular mass of $40\ \text{g}\ \text{mol}^{-1}$, Ar has a high kinetic energy which is large enough to destroy the sp^2 -bonded hexagonal structure of graphene. Besides, since Ar is easy to be

dissociated, it is of great efficiency that can etch multiple layers in a short time. As for hydrogen with much smaller mass (2 g mol^{-1}), it has relatively weaker ion bombardment effect which can be used to layer-by-layer etch for SLG with high precision. Hence, the thinning process was conducted by two different etching modes: one was the fast etching mode by Ar plasma, through which thick graphite flake could be etched into 5-layer graphene at a speed of 7-8 layers/min; the other was the fine mode of layer-by-layer etching with H_2 plasma.

By simply tuning the fast and fine etching modes, accurate control over the layer numbers of graphene

could be achieved. TLG, BLG, and SLG were obtained after three consecutive fine etching for 2 min, 1 min, and 1 min, respectively (Fig. 4). For all the obtained graphene with different layer numbers, it was successfully observed that large-area, uniform films covered all the domains across the sample. However, the defects level should not be ignored, as evidenced by the high I_D/I_G ratio of ~ 1.05 for SLG, although post annealing was introduced to effectively heal the defects produced by ion bombardment. Nevertheless, it is a less-invasive method that could be applicable in graphene-based device fabrication, since it has no obvious etching effect on the SiO_2/Si substrate.

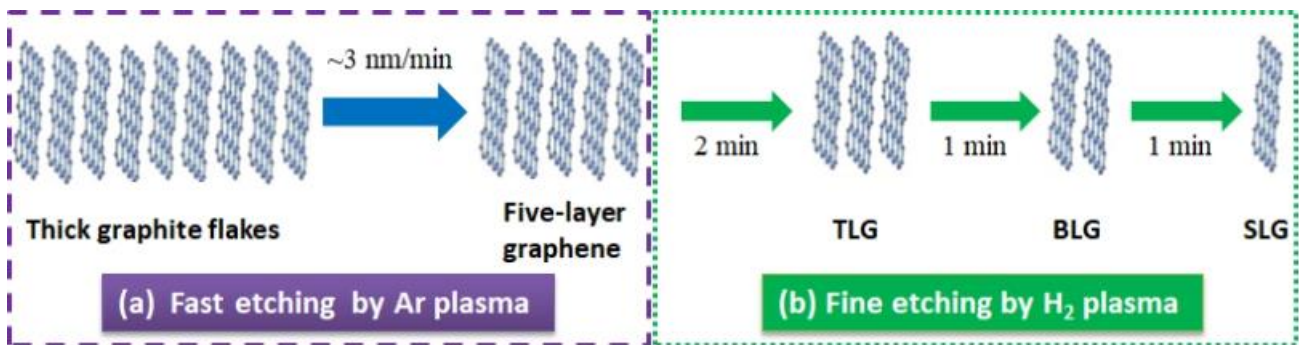


Fig. 4 Scheme of the plasma-thinning process from multiple-layer graphene to desired single-to-few layer graphene (1) fast etching by Ar plasma (b) fine etching by H_2 plasma (b)^[61]

2.3.2 Laser ablation

High-frequency laser has also found to be effective for the exfoliation of graphite^[62-63]. Han et al.^[60] found that FLG with 4 - 7 layers can be etched to SLG under reasonable laser power density.

To further enhance the layer-number controllability, Lin et al.^[63] demonstrated an accurate control of layer-by-layer thinning 5-layer CVD-graphene through picosecond laser radiation, as illustrated in Fig. 5. Since the photon energy of the laser (1.2 eV) was much higher than the van der Waals force between the graphene interlayers (0.17 eV), the peeling-off process was able to start from the grain boundaries of the CVD

graphene defects (Fig. 5(c)). Subsequently, the van der Waals force would be rapidly weakened along with the increase of the distance between the interacting grains and the adjacent layers, which finally led to the peel-off of the graphene. To obtain a specific layer-number graphene, the laser energy density should be adjusted to the level higher than the corresponding threshold, such as $\sim 1.0 \text{ J/cm}^2$ for SLG and $\sim 0.5 \text{ J/cm}^2$ for 4-layer graphene (Fig. 5(b)). By simply changing the pulse threshold energy, specific layer numbers from four to single layers were achieved in a controllable way.

It is worth notice that the formation energy of the C-C bond (3.7 eV) of the graphene is much higher than the photo energy. The graphene structure would

not be broken in the whole process. As a result, the obtained graphene exhibited very few defects, as evidenced by the small I_D/I_G value of less than 0.07. More importantly, it can be conducted in atmospheric condition in a simple, non-contact, and patternable way. Therefore, although graphene grain size was relatively small (normally about 1 μm , dependent on the CVD process), it is really an attracting method for the fabrication of graphene-based electronic devices.

In short, for the “top-down” methods based on the exfoliation of graphite, to achieve high-quality

graphene with controlled layer numbers, the key point is how to break the van der Waals force between the graphene interlayers in a proper way. On the one hand, no matter by ultrasonication, plasma, laser, or other energy, sufficient energy density is required to overcome the interaction between graphene layers (as presented in Fig. 5(b)). On the other hand, the energy applied should not be too high to destroy the graphene structure. Besides, effective measures should be taken to prevent the re-stacking of exfoliated GNS.

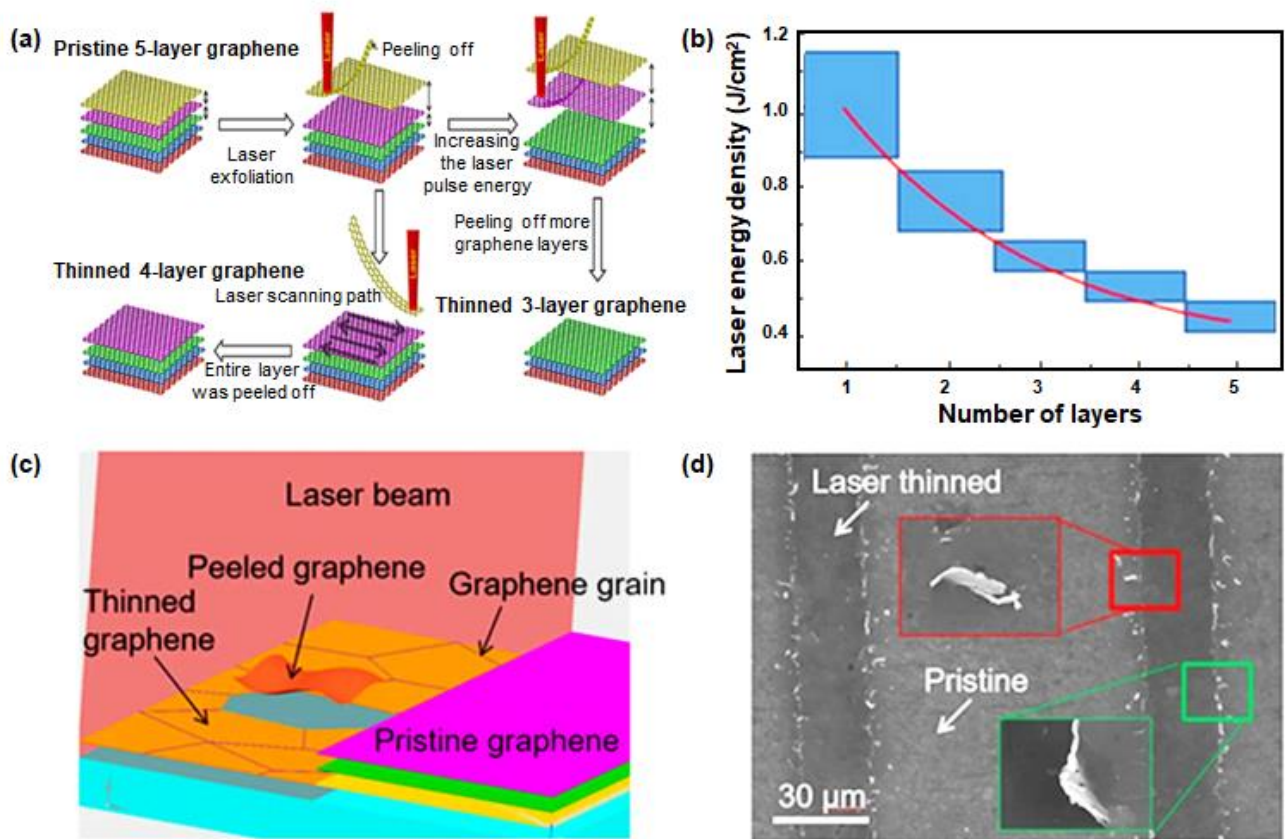


Fig. 5 (a) Schematic image of laser ablation process (b) Thresholds of the laser energy density for graphene with 1-5 layers (c) Scheme of the mechanism of laser ablation (d) SEM image of the graphene after laser ablation: the peeled-off graphene grains (marked in the red box) and the graphene grain residues (in the green box)^[63]

3 Layer-Number Controllable Synthesis of “Bottom-Up” Graphene

“Bottom-up” graphene usually refers to the large-area graphene film synthesized by CVD growth on metal substrates or epitaxial growth (EG) on SiC. It

has exhibited huge potentials in the application of future microelectronic industries, such as FETs, touch panels, and photovoltaic devices, especially the electrical interconnects in large-scale integrated circuits [25, 26, 30]. Since graphene with different layer numbers can enrich the adjustability in versatile applications, some efforts have already been devoted

to the preparation of large-area graphene with controlled thickness. The strategies, the carbon sources, the substrates, as well as the layer numbers,

and quality of the obtained graphene are summarized in **Table 1**.

Table 1 Methods for the layer-number control of graphene synthesized by “bottom-up” approaches

Methods	Strategies	Key parameters	Carbon sources	Substrates	Layer numbers	I_D/I_G	I_{2D}/I_G	Ref.
CVD	O ₂ -assisted CVD	O ₂ content	Propylene (C ₃ H ₆)	Ni	1~ few LG	<0.2	3~0.4	[64]
	Dual-metal substrates	Thickness of Co layer	CH ₄	Co/Cu	SLG, BLG, TLG, FLG	<0.1	>3, 0.4~0.8	[19]
	Layer-by-layer CVD	Growth time	CH ₄	Cu	SLG, BLG, TLG	~0	2.45, 1.04, 0.54	[21]
	Ion implantation CVD	Ion implant fluence	Carbon ions	Ni	FLG	0.21	1.4	[65]
	Ion implantation CVD	Ion implant fluence	Carbon ions	Ni/Cu	SLG, BLG	~0	>1.5, 0.5	[34]
	LDH-template CVD	MMA content	MMA	None	SLG, BLG, FLG	0.2 ~ 0.4	0.2~0.5	[66]
	Plasma-enhanced CVD	Growth temperature	C ₂ H ₂	Si/SiO _x	SLG, FLG	~1	1~2, 0.3~0.4	[67]
EG	Enclosure-assisted EG	Growth temperature	6H-SiC	SiC	FLG	0.06 ~ 0.10	2.63~3.13	[68]
	Layer-by-layer EG	In-situ synthesis	3C-SiC(001)	SiC	SLG, BLG, TLG	N/A	N/A	[69]
PVD	PVD	Annealing temperature & duration	Amorphous carbon (a:C)	Si	1~few	0.12~0.47	0.29~0.89	[70-71]
	PMS-PVD	Growth temperature	Graphite	Cu	SLG, FLG	0 ~ 0.5	3.57 ~2.0	[72]

Note: CVD = chemical vapor deposition; EG = epitaxial growth; PVD = physical vapor deposition; PMS-PVD = pulsed magnetron sputtering PVD; N/A = not available.

3.1 Chemical Vapor Deposition

CVD synthesis of graphene has been regarded as one of the most important techniques for high-quality graphene with large area and few defects^[30, 33, 73-75]. The typical process of CVD-graphene usually consists of three steps, i.e., carbon dissolving, thermal

annealing, and transfer process (usually by PMMA)^[33], as illustrated in Fig. 6. It is so complicated a system that the CVD growth of graphene tends to be influenced by many factors, at least including 1) the species, structure, and concentration of carbon sources^[76-78]; 2) the carbon solubility and crystallinity of the substrate^[21, 33, 79-82]; 3) the process parameters,

such as the gas flow ratio and rate, the growth and annealing temperature, the chamber pressure, the

deposition time, the cooling rate, and so on^[21, 23, 78, 83-84].

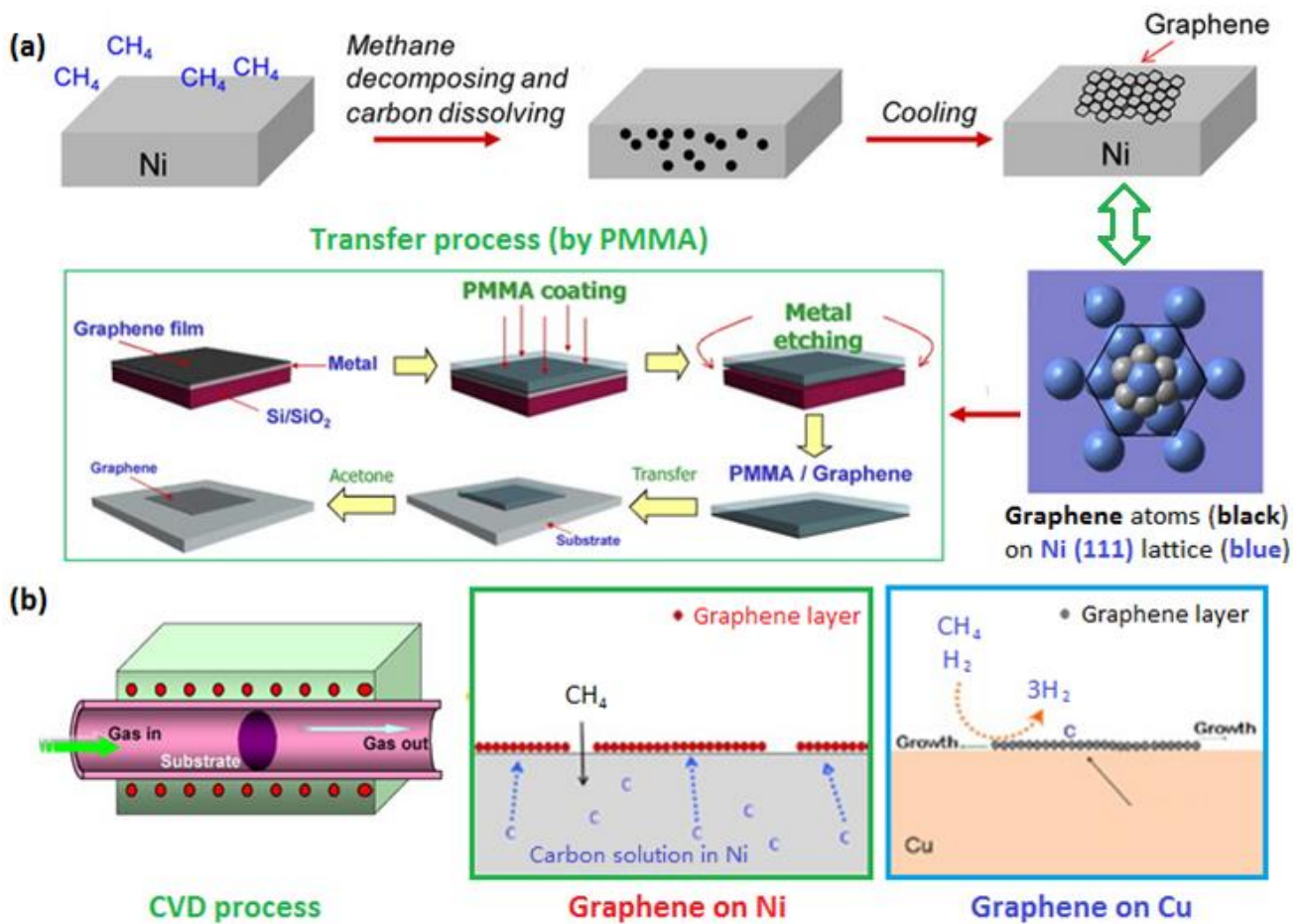


Fig. 6 Schematic image of the synthesis of graphene by CVD process (a). The differences in the mechanism of CVD-growth of graphene on Ni versus Cu (b)^[33]

Therefore, the CVD synthesis of high-quality graphene with controlled layer numbers is quite challenging. Nevertheless, some effective methods have been developed to solve this problem, such as introducing composite substrates, layer-by-layer CVD, ion-implantation CVD, template-assisted CVD, as well as plasma-enhanced CVD^[19, 21, 34, 66, 67].

3.1.1 Dual-metal catalyzed CVD

Studies on CVD growth of graphene have been extensively focused on two kinds of metal substrates with different carbon solubility. However, both of them have limitations in layer-number controllability. For the CVD growth of graphene based on the metals

with high solubility to carbon (e.g., Ni, Co, and Ru), which refers to precipitation process after surface segregation, the problem lies in the nonequilibrium-precipitation process which makes great challenges to tune the layer numbers of graphene. In contrast, for metals with low solubility to carbon (e.g., Cu, Pt, and Ge), the CVD growth of graphene tends to yield SLG rather than FLG since it follows a self-limiting surface mechanism^[19, 34].

Dual-metal substrates that combine the benefits of the two kind of metals with different carbon solubility have been found effective for enhancing the controllability of CVD growth^[19, 34].

In virtue of Co-coated Cu foil substrates, Lin et al.^[19] presented that the layer-number of CVD-

graphene can be precisely tuned by changing the thickness of the Co layers. The Co layer with moderate carbon solubility was designed as a carbon-dissolving place for graphene growth, while the Cu layer with low carbon solubility as carbon-rejecting layer. The carbon solubility of the composite substrate was successfully adjusted by regulating the thickness of the Co layer. As a result, uniform SLG, BLG, TLG, and FLG with few defects were obtained by varying the thickness of the Co layer to 80 nm, 130 nm, 205 nm, and 400 nm, respectively^[19]. It was found that the graphene thickness seemed insensitive to growth temperature and time. Besides, the obtained SLG films demonstrated high quality together with a high yield of 98%. The as-synthesized AB-stacked BLG and TLG were defects free and had a high surface coverage of 99%. In addition, the obtained graphene of 1 - 6 layers exhibited excellent layer-dependent properties, such as low electrical sheet resistance of 865 - 282 $\Omega \cdot \text{sq}^{-1}$, together with high transmittance at 550 nm of 97.3% - 84.9%.

However, it has been pointed out that the controllability of this method is still limited, since it is not easy to decouple the carbon adsorption and precipitation processes that are thermally driven and occur simultaneously^[34, 85].

3.1.2 Layer-by-layer CVD

Han et al.^[21] developed a layer-by-layer technique to prepare CVD-graphene with desired layer numbers in a precisely controllable way. This method is based on a novel two-heating zone CVD consisting of two-step procedures, as shown in Fig. 7(a-b). The first step was the growth of SLG as the conventional CVD did on Cu substrate with 10 sccm of CH_4 gas flow and 300 sccm of H_2 gas flow, at 1 Torr and 1040 °C for 10 min. The followed step was layer-by-layer growth of graphene on the as-grown monolayer under optimized experimental parameters. In virtue of the van der Waals epi-growth of 2D layered materials, layer-by-layer growth of monolayer graphene on the as-synthesized layer was successfully achieved through simply tuning the growth time. It turned out that BLG and TLG completely covered the previous layer at the growth time of 60 min and 120 min, respectively (Fig. 7(c)). The obtained SLG, BLG, and TLG were found in good quality with uniform thickness distribution and free of defects, as revealed by the Raman spectra in Fig. 7(d-e). More importantly, these outputs exhibited outstanding optical and electrical properties. The transmittance at 550 nm was recorded to be 97.4% for the SLG and down to 83.7% for 7-layer graphene. The sheet resistance was 723 Ω/sq for SLG and subsequently decreased with the increase of the layer numbers.

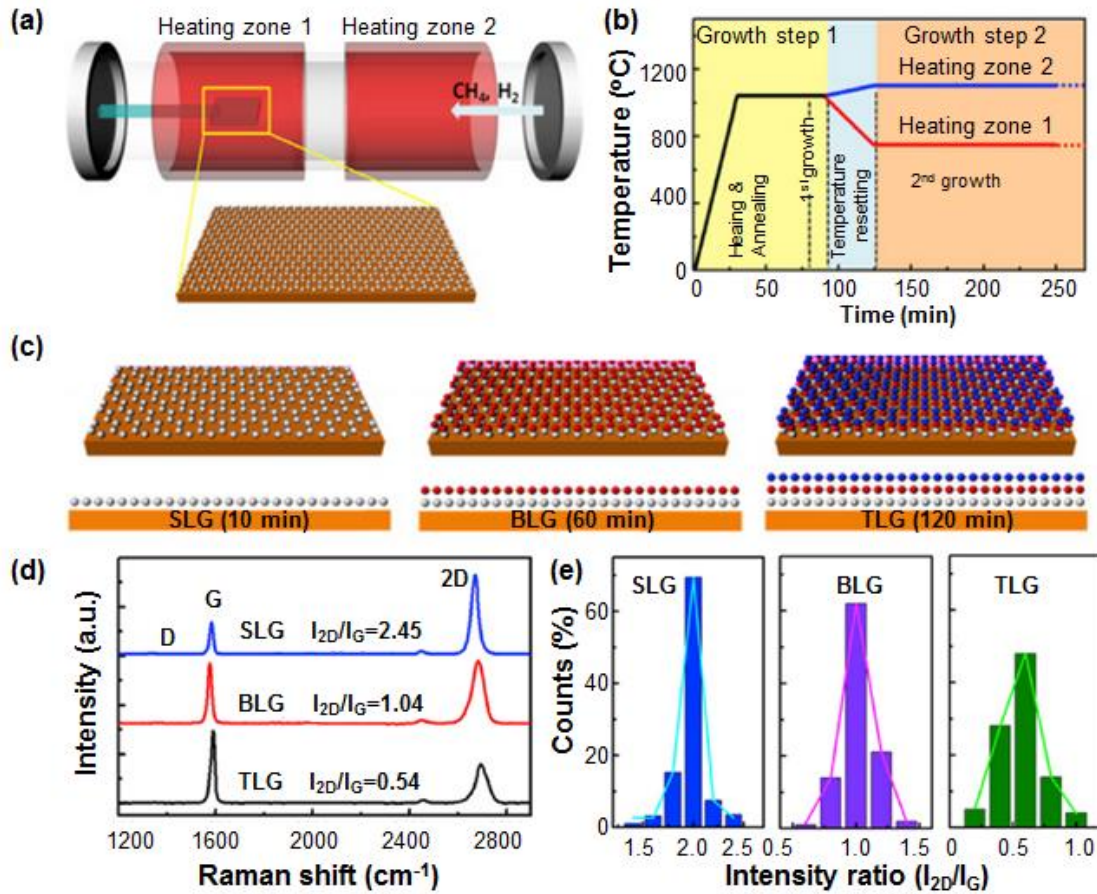


Fig. 7 (a-c) Schematic images of the layer-by-layer CVD-growth of graphene with controlled layer numbers: the two heating zones (a), the two growth steps (b) and the growth of SLG, BLG, and TLG (d-e) Raman spectra (d) and corresponding statistical histograms of the I_{2D}/I_G ratio (e) of the obtained SLG, BLG, and TLG on SiO_2/Si ^[21]

3.1.3 Ion implantation CVD

Ion implantation CVD refers to a pre-implantation of carbon species in the metal substrates, ahead of the high temperature annealing and quenching processes^[34, 65]. As a mature technology in the microelectronic industry, ion implantation has grand advantage in controlling the content of carbon atoms, which may significantly improve the controllability of graphene thickness. However, for the substrates of single metals such as Ni and Cu, it is not so satisfactory that the layer numbers of the obtained graphene are uneven, and the correlation between the carbon fluence and graphene thickness is not strictly followed^[86].

Aiming to enhance the controllability over the quality and layer numbers of CVD graphene, Wang et

al.^[34] adopted a dual-metal substrate, i.e., Ni-coated Cu foils (a 300-nm-thick Ni layer deposited on Cu foil). Since the final formation of graphene was on Cu-like alloy and the concentration of Ni was negligible, the graphene thickness was less sensitive to the thermodynamic process. Therefore, combining the advantages of the composite substrate and the precise implantation of carbon ions, it can be expected to achieve a stricter dependence of graphene thickness on the carbon fluence. In other words, it can be precisely controlled by simply tuning the dosage of carbon ions pre-implanted.

As illustrated in Fig. 8, carbon ions with predesigned fluence were implanted into the Ni layer of the Ni/Cu alloy. During the thermal treatment of CVD process, interdiffusion of Cu and Ni atoms occurred and carbon atoms were expelled to the

surface due to its poor solubility in Cu. Ultimately, uniform SLG and BLG were formed on the surface under the carbon ion implant fluence of 4×10^{15} and 8×10^{15} atoms·cm⁻², respectively. In addition, since the carbon ion was able to precipitate under steady temperature, defect healing of graphene could be achieved, which produced high-quality graphene with excellent crystalline and uniformity. The obtained

graphene turned out to be almost free of defects, as evidenced by the negligible presence of Raman D-band. Furthermore, the SLG and BLG films exhibited excellent carrier mobilities ($2000 \sim 4000$ cm² V⁻¹ s⁻¹ for holes and $1000 - 3500$ cm² V⁻¹ s⁻¹ for electrons), which indicates a bright application potential in graphene-based nano electronic devices.

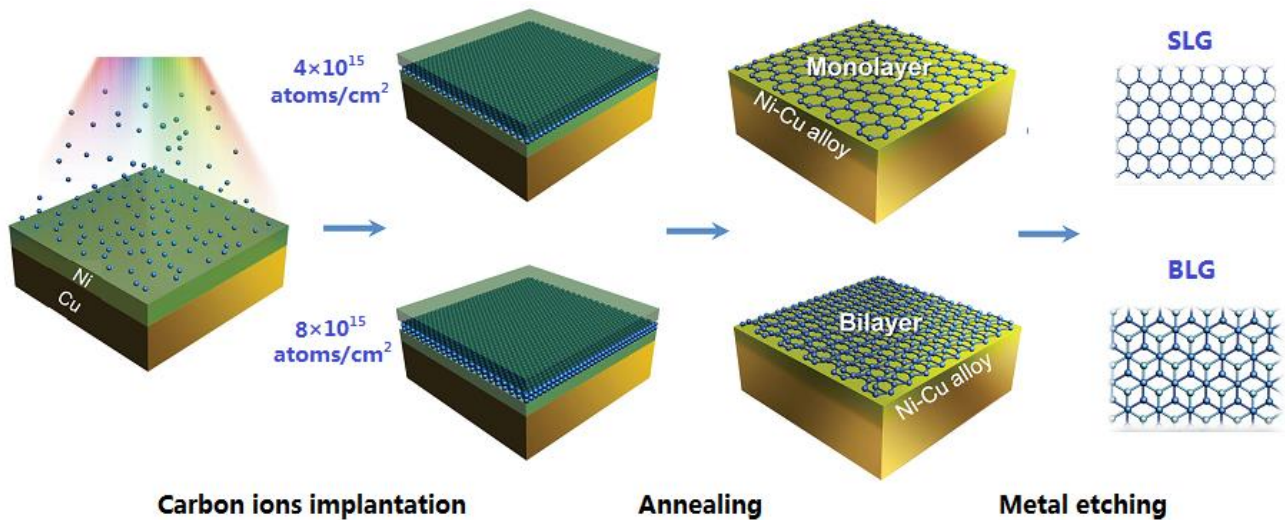


Fig. 8 Scheme of the synthesis of SLG and BLG by ion-implantation CVD on Ni/Cu substrate^[34]

3.1.4 Plasma-enhanced CVD

Since the traditional CVD-graphene requires too high growth temperature (usually $800 - 1000^{\circ}\text{C}$), plasma-enhanced CVD (PECVD) has attracted more and more attention as a solution to low-temperature growth of graphene ($\sim 600^{\circ}\text{C}$)^[87-88]. Different from the traditional CVD system, PECVD mainly consists of three component parts, including the gaseous system, the plasma generator system, and the vacuum heating system (Fig. 9(a)). According to the power source for plasma generation, the key component, the plasma generator, is usually categorized into three types, i.e., microwave plasma (~ 2.45 GHz), radio frequency plasma (~ 13.56 MHz), and direct current plasma. It is a catalyst-free synthesis method that can be applied to

the growth of graphene on not only metal substrates, but also dielectrics such as SiO₂ and Si^[89]. However, since it contains various kinds of species and reactions that greatly influence the morphology and thickness of graphene, the control of layer numbers is not an easy work^[89].

Recently, Muñoz et al.^[67] addressed the growth of graphene films with controlled thickness directly on Si/SiO_x wafers by a kind of microwave-PECVD method, using C₂H₂ as the carbon source. To better control the complicated reactions and interaction with the SiO_x, they adopted a two-step process to isolate the nucleation and growth stages of the graphene film. In the first step of graphene nucleation on Si/SiO_x, high-quality graphitic seeds were nucleated with controlled coverage and density. As shown in Fig. 9(b-c), the

nucleation density and grain size demonstrated well-controlled variation with the growth temperature, which made it possible to tune the thickness of graphene film by the growth temperature. In the second step, the nucleated seeds promoted the growth of the edge and finally the formation of graphene film. The typical AFM height of the obtained graphene film synthesized at 550 °C, 600 °C, and 650 °C turned out to be 0.7-1.0 nm (corresponding to SLG), 1.2-1.7 nm, and 1.5-2.2 nm (FLG), respectively. The SLG had a large grain size of over 300 nm and high crystallinity, leading to a remarkably low resistivity of 6.4×10^{-6}

Ω/m .

However, it must be noted that it is so complicated a process that requires accurate control of the interaction with the SiO_x . Besides, the quality is still under the thumb of the high nucleation density, which would lead to relatively low device performance. In addition, the growth rate is too low (below 10 nm min^{-1}) for industrial-scale production. Nevertheless, it proposed a low-temperature solution to the controllable synthesis of high-quality CVD graphene on dielectric materials.

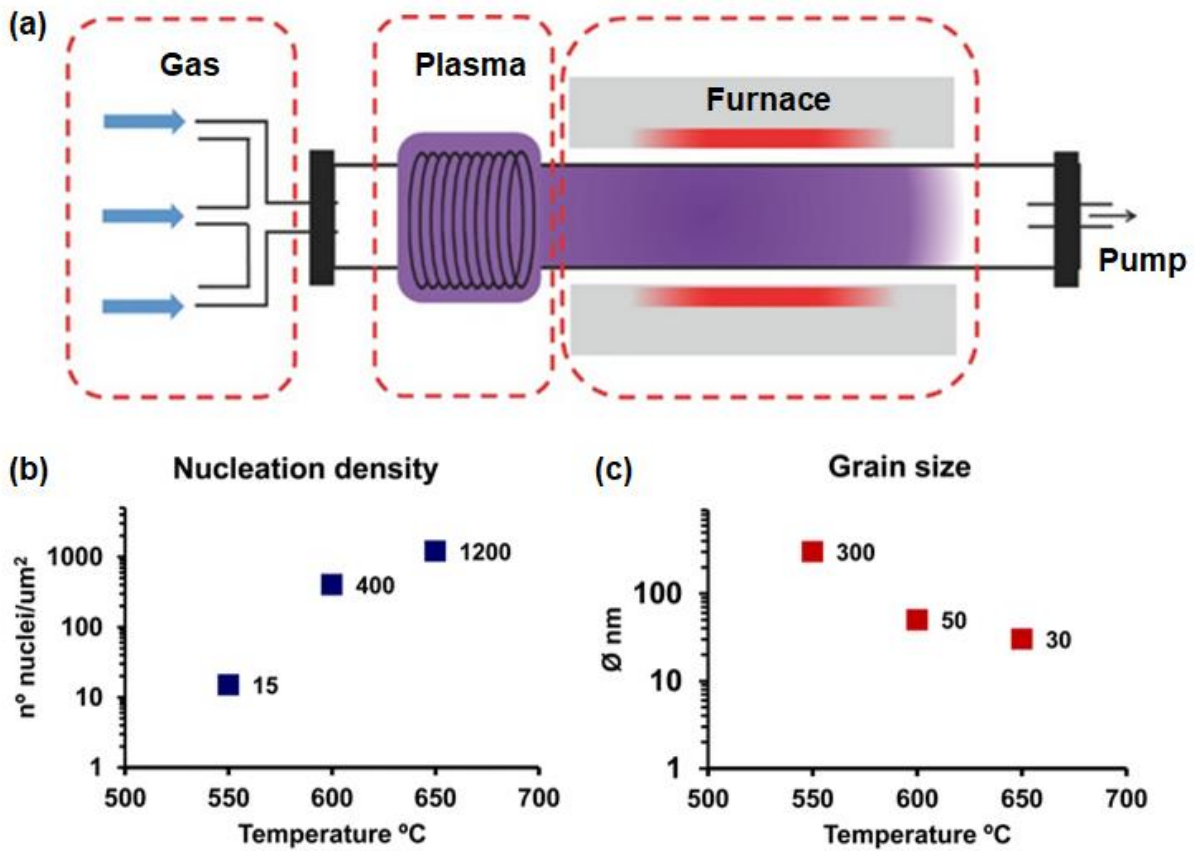


Fig. 9 (a) Schematic illustration of plasma-enhanced CVD^[89]. (b,c) The dependences of nucleation density (b) and grain size (c) on temperature^[67]

3.1.5 Template-assisted CVD

For the controllable growth of CVD graphene, Sun et al.^[66] designed a novel 2D template, named layered double hydroxides (LDH), for the synthesis of graphene nanosheets in the interlayer galleries.

The LDH templates were prepared as follows: 1) Dissolve the mixture of $\text{Mg}(\text{OH})_2 \cdot 6\text{H}_2\text{O}$ and $\text{Al}(\text{OH})_3 \cdot 9\text{H}_2\text{O}$ in deaerated water; 2) Add methyl methacrylate (MMA) and dodecyl sulfonate (DSO) to form an emulsion; 3) Add NaOH into the emulsion and reacted at 80 $^\circ\text{C}$ for 8 h; 4) Dry the precipitate filtered at 50 $^\circ\text{C}$ for 10 h. Here, MMA acted as the

carbon source, whereas the role of the DSO was to support the layers and provide space for MMA.

Subsequently, the intercalated MMA was calcined into graphene by H_2/Ar at 900 °C for 2 h. As shown in Fig. 10, it was believed that the confined 2D interlayer of LDH provided suitable space for the formation of graphene. By adjusting the quantity of MMA intercalated in the layered precursor, SLG, BLG, and FLG were satisfactorily synthesized in the interlayer.

Finally, GNS dispersion was easily obtained by dissolving the metal oxide phase in hydrochloric acid.

Notably, the first advantage of this method lies in that it avoids the complicated transfer process of traditional metal-catalyzed CVD method. Besides, since the LDH precursor can be made from cheap materials that are readily available, it is cost-efficient and easy to scale-up. Although the defects cannot be ignored according to the strong Raman D-bands, and the properties such as electrical conductivity need to be further evaluated. It surely provides another option for the layer-number controllable CVD synthesis of graphene without transfer process.

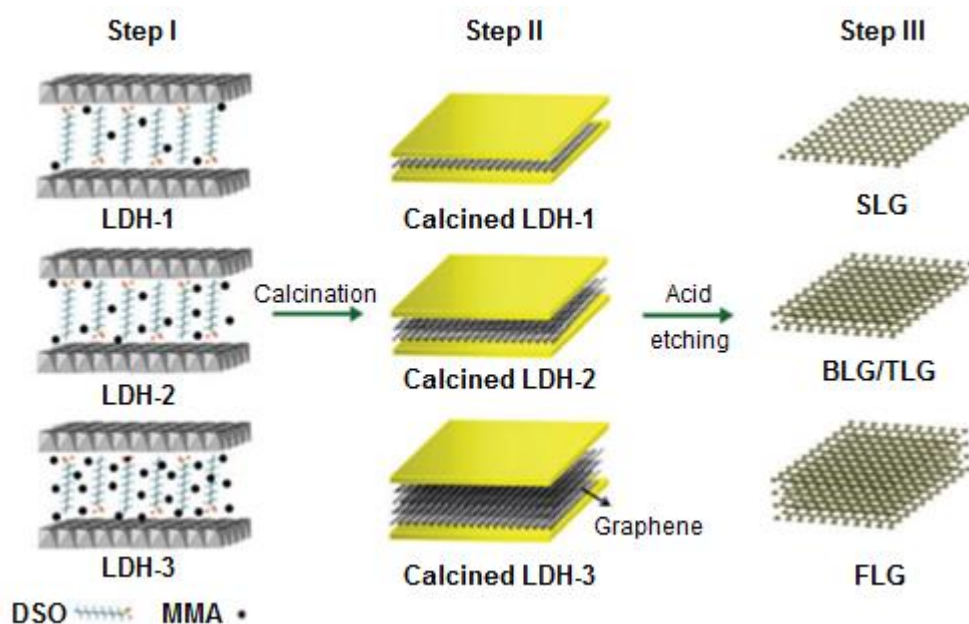


Fig. 10 Scheme for the CVD synthesis of graphene with controlled layer numbers by template of layered double hydroxides (LDH) with different molar ratios of MMA to dodecyl sulfonate (DSO), marked as LDH-1 (1.2), LDH-2 (3.2), and LDH-3 (8.0), respectively^[66]

3.2 Epitaxial Growth on SiC

The biggest shortage of CVD graphene lies in the transfer process from the metal substrates to the desired substrates, which brings many defects and impurities that may deteriorate the final properties. In fact, for successful electronic applications, graphene must be synthesized on semiconductive or insulative substrates, such as silicon wafers and glasses^[90]. Hence, much attention has been paid to the epitaxial growth of graphene on the semiconductive SiC, which can be directly used in high power, high frequency, and high

temperature devices such as LEDs^[91-92].

“Epitaxial growth” means the growth of a crystalline layer on a crystalline substrate which follows the structure of the substrate. Since Si has a higher vapor pressure than C in SiC, large-area and high-quality graphene can be achieved by thermal decomposition of SiC single crystal under a high degree of vacuum. It was reported that the domain area of epitaxial graphene on SiC could be as large as 200 $\mu m \times 200 \mu m$, which is much larger than that prepared by other methods^[93-94].

However, many factors have been found to influence

the growth and properties of epitaxial graphene. First of all, the two polar faces of SiC (i.e., C-face and Si-face) exhibit quite different properties during the growth of graphene. The Si face has advantages in the thickness control and homogeneous growth of graphene due to the slow growth rate on the Si face, but the low charge carrier mobility of the obtained graphene is not satisfactory^[68, 92]. As for the C face, although the electronic properties of the obtained graphene can be close to the mechanically exfoliated graphene films, the thickness of C-face graphene increases sharply with the elevating of graphitization temperature^[95]. Besides, the thickness of the epitaxial graphene varies with many process parameters, such as the vacuum conditions, the growth temperature, and its duration, and so on^[96-97]. Therefore, it is not easy to obtain epitaxial graphene on SiC with desired layer numbers and high quality in a controllable way.

For a better controllability over the thickness of epitaxial graphene, Hu et al.^[68] introduced a graphite enclosure into the epitaxial growth process on the C-face of 6H-SiC. The graphite enclosure was designed to provide a relatively high and dynamically balanced Si partial pressure, so as to slow down the growth rate and enhance controllability of graphene growth. Specifically, the 6H-SiC was firstly etched by hydrogen at 1600 °C in H₂ 80 L/min and C₃H₈ 5 mL/min for 7 min. Then, the H₂-etched SiC samples were put into the graphite enclosure for epitaxial growth under $\sim 10^{-3}$ mbar. As the graphitization temperature elevated from 1300 to 1600 °C, the thickness of epitaxial graphene exhibited a slow climb from 0.4 to 3.8 monolayers. That is to say, the layer numbers of the epitaxial graphene became tunable with the help of the graphite enclosure. In addition, along with the elevation of the growth temperature, the stacking, homogeneity, and continuity, as well as the crystalline quality were improved a lot. Therefore, the obtained graphene exhibited quite good quality, as evidenced by the homogeneous coverage, large domain size of ~ 3 μm , and small Raman I_D/I_G ratio

of 0.06.

It should be mentioned that more accurate control over the thickness of epitaxial graphene has been realized in the lab, with the aid of some advanced instruments^[69, 98]. For example, Aristov et al.^[69] demonstrated the layer-by-layer synthesis of epitaxial SLG, BLG, and TLG on 3H-SiC/Si(001) wafers, utilizing LEED and high-resolution spectroscopy equipped with fast dynamic-XPS synchrotron facilities. The epitaxial growth of graphene occurred in the fast dynamic-XPS stations, while its thickness was real-time controlled by the micro-spot XPS according to the C1s core level spectra. More importantly, the synthesis procedure would stop once a desired layer numbers of graphene was gained. Therefore, the layer-by-layer growth of graphene can be achieved “automatically”, without following a particular recipe of the process parameters as the traditional epitaxial-growth method does.

3.3 Physical Vapor Deposition

Physical vapor deposition (PVD) is a low-cost, convenient, and scalable method for fabricating large-area uniform films^[99-100]. Thus, it is of great potential to study the controllable preparation of graphene in this field^[72, 101].

Narula et al.^[70, 71, 102] investigated the PVD growth of graphene on Cu using radio frequency (RF) and direct current (DC) sputtering technology. The method they developed consists of 4 steps: 1) deposition of amorphous carbon (a-C) thin film (12 - 60 nm) on Si substrate by RF sputtering; 2) deposition of Cu nanoparticles (800 nm) on the as-deposited a-C films by DC sputtering; 3) growth of graphene on the top of the Cu film under necessary sputtering energy by the catalysis of the sputtered Cu thin film; 4) annealing in hydrogen environment at 1020 °C for 50 min under a low pressure of 1 Torr^[103]. Based on a systematic study of the complicated factors, they suggested that relatively lower annealing temperature and shorter duration are

more helpful for lowering down the thickness of the obtained graphene. When the annealing temperature decreased from 1020 °C to 920 °C for the same duration of 50 min, the I_{2D}/I_G ratio increased from 0.9 to 1.6, which indicated the presence of multi-layer graphene with more than 10 layers and FLG with 3-9 layers, respectively. After a further reduction of the duration time to 20 min at 920 °C, the I_{2D}/I_G ratio increased to 2.6, indicating the presence of SLG^[102]. Therefore, graphene with different layers can be obtained by carefully adjusting the annealing temperature and duration.

To further improve the quality of PVD graphene films, Vijayaraghavan et al.^[72] introduced a so-called pulsed magnetron sputtering (PMS) technique. Compared with DC and RF sputtering, PMS exhibited higher adatom mobility, surface diffusion, and deposition rate. The PMS of graphite was carried out in an argon atmosphere with high-purity of 99.999%, under a base pressure of 4.5×10^{-4} mTorr. Carbon atoms from the graphite were sputtered on to a Cu foil and deposited to form graphene films under different growth temperature. It was found that the thickness of the graphene film was directly influenced by the deposition temperature. As the deposition temperature increased from 700 to 920 °C, the Raman I_{2D}/I_G ratio increased almost linearly from 0.40 to 3.57, which suggested the formation of graphene with 3-4 layers to single layer, respectively. The corresponding Raman D peaks exhibited an obvious

decrease and almost disappeared at 920 °C. That is to say, graphene with desired thickness from few layers to single layer can be controllably prepared by adjusting the deposition temperature. Besides, the obtained SLG had such a high quality that the defects level was quite low. Therefore, this kind of method with industrial scalability should be paid more attention to and further explored.

4 Applications of Graphenes with Different Layers

The potential applications of graphene have been reviewed by many outstanding works from various aspects, as illustrated in Table 2. It is noteworthy that the application areas can be further expanded when it is introduced into various other materials such as polymers, ceramics, and metals^[2, 104-107]. However, the respective advantages of graphene with different layers in properties and applications have not been systematically presented. Some attracting potentials of SLG, BLG, and FLG in the emerging industries are summarized, such as new energy materials, sensors, bio-materials, electronics, composites, and so on, as shown in Fig. 11^[108-114]. In Fig.11, the seven number-marked application areas refer to graphene as a whole, especially for SLG. The yellow dash lines highlight the advantageous fields of BLG and FLG over SLG.

Table 2 Literatures on the applications of graphene-based materials

Authors	Year	Graphene	Applications	Refs
Choi et al.	2010	Graphene with single to few layers	Field emission, gas and bio sensors, FET, transparent electrodes, battery	[115]
Zhang et al.	2013	CVD graphene	OPV cells, FETs	[33]
Liu et al.	2014	Graphene and its derivatives	Fuel cells	[110]
Quesnel et al.	2015	Graphene and its derivatives	Energy (e.g., Photovoltaics)	[104]
Palaniselvam et al.	2015	Graphene-based 2D materials	Supercapacitors (as potential electrodes)	[105]

Maharubin et al.	2016	Graphene and its derivatives	Fuel cells, solar cell, thermoelectric devices, supercapacitors, lithium-ion batteries.	[116]
El-Kady et al.	2016	Graphene with 0D to 3D structures	Energy storage	[117]
Li et al.	2016	2D graphene on various substrates by PECVD	FETs, photovoltaic devices, supercapacitors, sensors and charge trapping memory	[89]
Nag et al.	2018	Graphene	Sensors	[118]
Rowley-Neale et al.	2018	Reduced oxidized graphene	Electrochemical sensors and associated applications	[119]
Loh et al.	2010	Reduced oxidized graphene	Biological applications, transparent conductors	[120]
Abbasi et al.	2016	Graphene and its derivatives	Biomedical applications, transistors	[108]
Shareena et al.	2018	Graphene and its derivatives	Biomedical applications	[109]
Liu et al.	2015	Graphene-based membranes	Membranes for molecular separation	[121]
Huang et al.	2015	Nanoporous graphene and its derivatives	Membranes for molecular separation	[122]
Lin et al.	2016	Large-area graphene	Membrane separation	[123]
Xu et al.	2018	Functionalized CNTs and graphene	Heavy metal adsorption from water	[124]
Wassei et al.	2010	Graphene-based materials	Transparent conductor	[125]
Kuilla et al.	2010	Graphene and its derivatives	Composites	[106]
Phiri et al.	2017	Graphene and its derivatives	Composites	[107]
Papageorgiou et al.	2017	Graphene and its derivatives	Composites	[2]

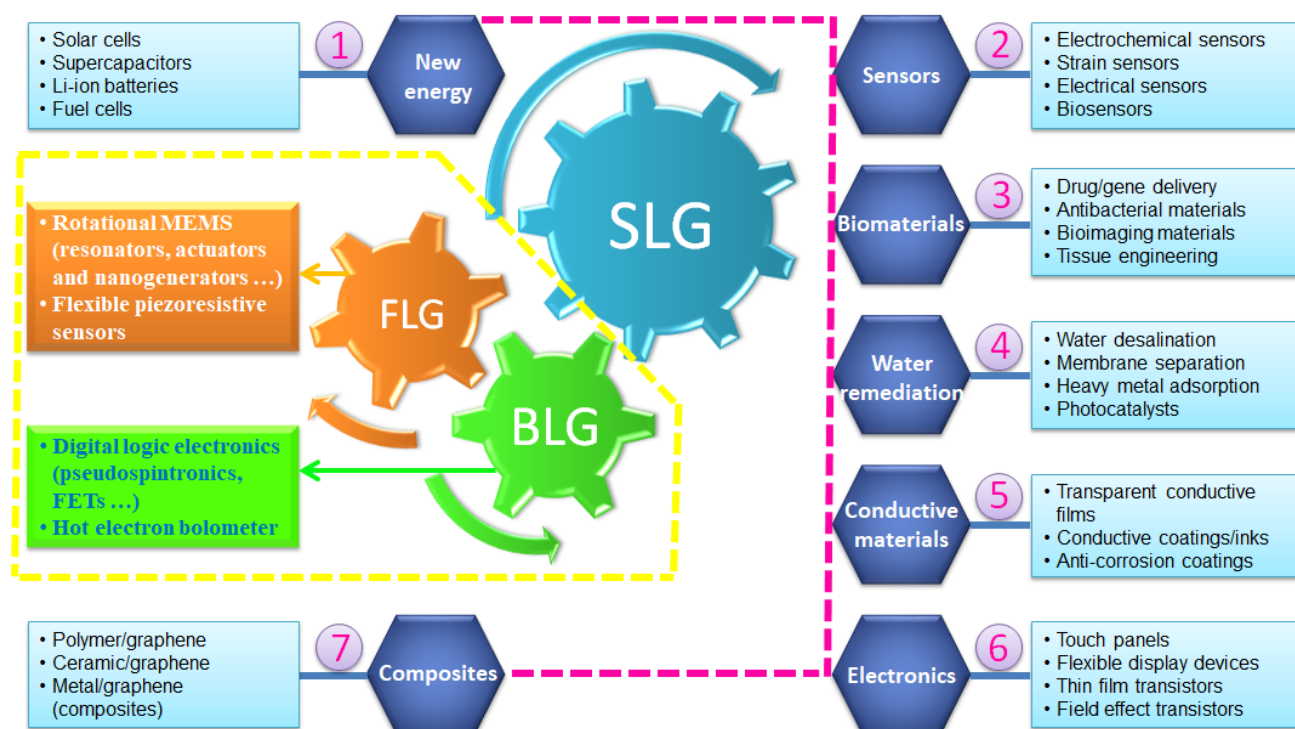


Fig. 11 Potential applications of graphene

First of all, compared with BLG, TLG, or graphene with more layers, SLG usually exhibits better performance in many properties such as electrical and thermal conductivity, optical and mechanical properties, and so on^[126]. Therefore, SLG has demonstrated great potentials in many fields, such as semi-transparent organic solar cells, transparent conductive anodes, organic light-emitting diodes and FETs, as well as large-scale integration^[110, 127]. Nevertheless, there still exist some limitations on the application of SLG. For example, the linear band structure of SLG brings great troubles for its application in digital logic transistors, which exhibits a high off-state leakage and non-saturating drive currents due to the lack of electronic bandgap^[128]. In other words, graphene with two or more layers has their own advantages for versatile application potentials owing to their unique properties.

Secondly, as the simplest multilayer graphene, BLG shares not only the merits of SLG such as high electron mobility, mechanical strength and flexibility^[129], but also those of other multilayer graphene, such as band-gap opening and coherent phonons, which leads to some unique and attractive potentials^[17]. Here are some typical examples: 1) Owing to the tunable bandgap, BLG has exhibited many advantages, e.g., unique electrical characteristic of slowly increased conductivity with the increase of charge density, unipolar p-type MOSFET behavior and high on/off current-ratio ($10^4 - 10^7$) at room temperature, in digital logic applications such as FETs, pseudo-spintronics and other electronics^[130-131]. 2) BLG has tunable Fano resonance for the phonon mode in infrared spectra, which can be used as hot electron bolometer. It was reported that the BLG-based hot electron bolometer has much lower noise equivalent power and 3-5 orders of magnitude larger intrinsic speed, compared with the commercial silicon bolometer^[129]. 3) BLG has exhibited similar effective Young's modulus to that of SLG, but higher levels of reinforcement in nanocomposites

according to the result of strain-induced Raman 2D-band shift. Notably, there was no slippage observed between the interlayers of BLG which was found for TLG and FLG and would lead to a decrease in the Young's modulus of the composites^[132]. Therefore, BLG, rather than SLG, may be the best choice for improving the mechanical properties of graphene-based nanocomposites.

Third, FLG has also received many interests from fundamental research to technological development: 1) The large structural anisotropy makes FLG a favorable candidate for the study of the rich physics from 3D to 2D systems^[133]. 2) Compared with SLG and BLG, FLG has exhibited some unique advantages in the applications of solar cells and micro-electromechanical systems (MEMS)^[134-138]. Li et al.^[134] found that the power conversion efficiency of the solar cell fabricated with 4-layer graphene is two times larger than that with SLG. Besides, since the friction decreases monotonically as the layer-number of graphene increases (Fig. 1(d))^[139], FLG demonstrates better wear resistance than SLG as tested in rotating MEMS which indicates a longer service life^[140-141]. 3) FLG may exhibit better mechanical, thermal, and other properties under some circumstances^[142-144]. For example, it was revealed that 7-layer CVD graphene may have higher thermal conductivity than graphene of 2-3 layers, due to the decrease of defects under higher growth temperature^[142]. Liang et al.^[143] found that for the graphene/polypropylene composites, FLG with 6-10 layers has better impact fracture toughness than that with 1-6 layers, since it can store more impact deformation energy. Moreover, in flexible piezoresistive sensors, FLG demonstrated better sensor sensitivity which rose from 0.051 to 11.1 kPa⁻¹ as the layer numbers of graphene increased from 4 to 11^[144]. It can be predicted that the few-layer graphene with intrinsic and stable electrical conductivity and high dispersity in membrane-forming polymer solutions would be

potentially used as vital additives in the highly sensitive sensing membranes for the fabrication of advanced long-life heavy-metal ion sensors^[145-150].

In short, graphene with different layer numbers has exhibited respective advantages in both the physicochemical properties and potential applications. The preparation of high-quality graphene with well-controlled layer numbers will greatly enrich the commercial value and prospects.

5 Conclusions and Outlook

In summary, the status on layer-number controllable synthesis of graphene has been elaborated based on the two complementary approaches of “top-down” and “bottom-up”, and the applications of graphene with different layer numbers. For “top-down” approaches, it is still of great challenge to prepare high-quality graphene with controlled layer numbers. However, some advances are quite enlightening:

1) Employing highly-diffusive supercritical CO₂ as dispersion media has demonstrated its improvement in layer-number controllability;

2) Thinning by laser or plasma are beneficial for the precise control of graphene layers.

For “bottom-up” approaches, the situation seems more optimistic:

1) Some effective techniques have been developed for precise control in the thickness of CVD graphene on metal substrates, such as introducing dual-metal substrates, layer-by-layer CVD, ion-implantation CVD;

2) Two-step plasma-enhanced CVD provides a good solution to the low-temperature growth of graphene on various substrates, especially dielectrics for application in electronics;

3) Template-assisted CVD (by layered-double-hydroxides) provides another option for the layer-number controllable CVD synthesis of graphene without transfer process;

4) In terms of thermal epitaxial growth, the introduction of graphite enclosure, which provides a

relatively high partial-pressure of Si in dynamical balance, significantly enhances the controllability on its thickness and quality;

5) PMS-PVD should be paid more attention to and further explored, since it may be a low-cost and scalable solution for industrial production of high-quality graphene.

Although great challenges still exist in the scalable fabrication of high-quality graphene with controlled and homogeneous thickness, the above-reviewed significant progresses in the controllable preparation of graphene have shown us a brighter future. Considering the huge application potentials of graphene and the respective advantages of graphene with different layer numbers, more efforts should be devoted to the layer-number controllable preparation of high-quality graphene, as well as its feasibility of industrial production. We have every reason to believe that more and more achievements would be made in this field in the near future.


Author contributions

Y. B. Xie and M. R. Huang contributed equally.

Acknowledgements

Xin-Gui Li and Mei-Rong Huang are grateful to Professor Hiroshi Imahori, Professor Tomokazu Umeyama, Professor Tomohiro Higashino, and Ms. Naoko Nishiyama at Department of Molecular Engineering, Kyoto University, Japan for their assistance.

ORCID IDs

Yun-Bin Xie  <https://orcid.org/0000-0002-6577-5718>

Mei-Rong Huang  <https://orcid.org/0000-0002-8563-7910>

Xin-Gui Li  <https://orcid.org/0000-0001-7750-7158>

References

- [1] Singh V, Joung D, Zhai L, et al. Graphene based materials: past, present and future. *Progress in Materials Science*, 2011, 56(8): 1178-1271. DOI: 10.1016/j.pmatsci.2011.03.003.
- [2] Papageorgiou D G, Kinloch I A, Young R J. Mechanical properties of graphene and graphene-based nanocomposites. *Progress in Materials Science*, 2017, 90: 75-127. DOI: 10.1016/j.pmatsci.2017.07.004.
- [3] Li X G, Tao Y, Li F R, et al. Efficient preparation and characterization of functional graphene with versatile applicability. *Journal of Harbin Institute of Technology (New Series)*, 2016, 23(3): 1-29. DOI: 10.11916/j.issn.1005-9113.2016.03.001.
- [4] Fan Y H, Hu G W, Yu S Q, et al. Recent advances in TiO₂ nanoarrays/graphene for water treatment and energy conversion/storage. *Science China Materials*, 2019, 62(3): 325-340. DOI: 10.1007/s40843-018-9346-3.
- [5] Li X G, Huang M R, Duan W, et al. Novel multifunctional polymers from aromatic diamines by oxidative polymerizations. *Chemical Reviews*, 2002, 102(9): 2925-3030. DOI: 10.1021/cr010423z.
- [6] Liao Y Z, Li X G, Kaner R B. Facile synthesis of water-dispersible conducting polymer nanospheres. *ACS Nano*, 2010, 4(9): 5193-5202. DOI: 10.1021/nn101378p.
- [7] Liao Y Z, Strong V, Wang Y, et al. Oligotriphenylene nanofiber sensors for detection of nitro-based explosives. *Advanced Functional Materials*, 2012, 22(4): 726-735. DOI: 10.1002/adfm.201102013.
- [8] Li X G, Liu Y W, Huang M R, et al. Simple efficient synthesis of strongly luminescent polypyrrole with intrinsic conductivity and high carbon yield by chemical oxidative polymerization of pyrene. *Chemistry-A European Journal*, 2010, 16(6): 4803-4813. DOI: 10.1002/chem.200902621.
- [9] Li X G, Liao Y Z, Huang M R, et al. Ultra-sensitive chemosensors for Fe(III) and explosives based on highly fluorescent oligofluoranthene. *Chemical Science*, 2013, 4(5): 1970-1978. DOI: 10.1039/C3SC22107E.
- [10] Edwards R S, Coleman K S. Graphene synthesis: relationship to applications. *Nanoscale*, 2013, 5(1): 38-51. DOI: 10.1039/c2nr32629a.
- [11] Zhang Y Y, Gu Y T. Mechanical properties of graphene: effects of layer number, temperature and isotope. *Computational Materials Science*, 2013, 71: 197-200. DOI: 10.1016/j.commatsci.2013.01.032.
- [12] Tu Z Q, Liu Z C, Li Y F, et al. Controllable growth of 1-7 layers of graphene by chemical vapour deposition. *Carbon*, 2014, 73: 252-258. DOI: 10.1016/j.carbon.2014.02.061.
- [13] Lee C, Wei X D, Li Q Q, et al. Elastic and frictional properties of graphene. *Physica Status Solidi B-Basic Solid State Physics*, 2009, 246(11-12): 2562-2567. DOI: 10.1002/pssb.200982329.
- [14] Zhong W R, Zhang M P, Ai B Q, et al. Chirality and thickness-dependent thermal conductivity of few-layer graphene: a molecular dynamics study. *Applied Physics Letters*, 2011, 98(11): 113107. DOI: 10.1063/1.3567415.
- [15] Shiu H W, Chang L Y, Lee K H, et al. Graphene as tunable transparent electrode material on GaN: layer-number-dependent optical and electrical properties. *Applied Physics Letters*, 2013, 103(8): 081604. DOI: 10.1063/1.4818787.
- [16] Costa S D, Weis J E, Frank O, et al. Effect of layer number and layer stacking registry on the formation and quantification of defects in graphene. *Carbon*, 2016, 98: 592-598. DOI: 10.1016/j.carbon.2015.11.045.
- [17] Rozhkov A V, Sboychakov A O, Rakhmanov A L, et al. Electronic properties of graphene-based bilayer systems. *Physics Reports*, 2016, 648: 1-104. DOI: 10.1016/j.physrep.2016.07.003.
- [18] McCann E, Koshino M. The electronic properties of bilayer graphene. *Reports on Progress in Physics*, 2013, 76(5): 056503. DOI: 10.1088/0034-4885/76/5/056503.
- [19] Lin T Q, Huang F Q, Wan D Y, et al. Self-regulating homogenous growth of high-quality graphene on Co-Cu composite substrate for layer control. *Nanoscale*, 2013, 13(5): 5847-5853. DOI: 10.1039/c3nr33124e.
- [20] Parviz D, Irin F, Shah S A, et al. Challenges in liquid-phase exfoliation, processing, and assembly of pristine graphene. *Advanced Materials*, 2016, 28(40): 8796-8818. DOI: 10.1002/adma.201601889.
- [21] Han J, Lee J Y, Yeo J S. Large-area layer-by-layer controlled and fully bernal stacked synthesis of graphene. *Carbon*, 2016, 105: 205-213. DOI: 10.1016/j.carbon.2016.04.039.
- [22] Wu Z S, Ren W C, Gao L B, et al. Synthesis of high-quality graphene with a pre-determined number of layers. *Carbon*, 2009, 47(2): 493-499. DOI: 10.1016/j.carbon.2008.10.031.
- [23] Liu W, Kraemer S, Sarkar D, et al. Controllable and rapid synthesis of high-quality and large-area Bernal stacked bilayer graphene using chemical vapor deposition. *Chemistry of Materials*, 2014, 26(2): 907-915. DOI: 10.1021/cm4021854.
- [24] Lin L, Peng H L, Liu Z F. Synthesis challenges for graphene industry. *Nature Materials*, 2019, 18: 520-524. DOI: 10.1038/s41563-019-0341-4.
- [25] Englert J M, Hirsch A, Feng X, et al. Chemical methods for the generation of graphenes and graphene nanoribbons.

- Angewandte Chemie-International Edition, 2011, 50(37): A17-24.
- [26]Ciesielski A, Samori P. Graphene via sonication assisted liquid-phase exfoliation. Chemical Society Reviews, 2014, 43(1): 381-398. DOI: 10.1039/C3CS60217F.
- [27]Johnson D W, Dobson B P, Coleman K S. A manufacturing perspective on graphene dispersions. Current Opinion in Colloid & Interface Science, 2015, 20(5-6): 367-382. DOI: 10.1016/j.cocis.2015.11.004.
- [28]Mohan V B, Lau K-t, Hui D, et al. Graphene-based materials and their composites: a review on production, applications and product limitations. Composites Part B-Engineering, 2018, 142: 200-220. DOI: 10.1016/j.compositesb.2018.01.013.
- [29]Du Y C, Huang L J, Wang Y X, et al. Recent developments in graphene-based polymer composite membranes: preparation, mass transfer mechanism, and applications. Journal of Applied Polymer Science, 2019, 136(28): 47761. DOI: 10.1002/app.47761.
- [30]Pang J B, Mendes R G, Wrobel P S, et al. Self-terminating confinement approach for large-area uniform monolayer graphene directly over Si/SiO_x by chemical vapor deposition. ACS Nano, 2017, 11(2): 1946-1956. DOI: 10.1021/acsnano.6b08069.
- [31]Yazdi G R, Vasiliauskas R, Iakimov T, et al. Growth of large area monolayer graphene on 3C-SiC and a comparison with other SiC polytypes. Carbon, 2013, 57: 477-484. DOI: 10.1016/j.carbon.2013.02.022.
- [32]Wang F, Chen G R, Li W, et al. Layer controllable graphene using graphite intercalation compounds with different stage numbers through Li conversion reaction. Advanced Materials Interfaces, 2016, 3(3): 201500496. DOI: 10.1002/Admi.201500496.
- [33]Zhang Y, Zhang L Y, Zhou C W. Review of chemical vapor deposition of graphene and related applications. Accounts of Chemical Research, 2013, 46(10): 2329-2339. DOI: 10.1021/ar300203n.
- [34]Wang G, Zhang M, Liu S, et al. Synthesis of layer-tunable graphene: a combined kinetic implantation and thermal ejection approach. Advanced Functional Materials, 2015, 25(24): 3666-3675. DOI: 10.1002/adfm.201500981.
- [35]Wei D C, Liu Y Q. Controllable synthesis of graphene and its applications. Advanced Materials, 2010, 22(30): 3225-3241. DOI: 10.1002/adma.200904144.
- [36]Xue Y Z, Wu B, Bao Q L, et al. Controllable synthesis of doped graphene and its applications. Small, 2014, 10(15): 2975-2991. DOI: 10.1002/smll.201400706.
- [37]Ferrari A C, Basko D M. Raman spectroscopy as a versatile tool for studying the properties of graphene. Nature Nanotechnology, 2013, 8(4): 235-246. DOI: 10.1038/nnano.2013.46.
- [38]Kumar R, Singh R K, Singh D P, et al. Laser-assisted synthesis, reduction and micro-patterning of graphene: recent progress and applications. Coordination Chemistry Reviews, 2017, 342: 34-79. DOI: 10.1016/j.ccr.2017.03.021.
- [39]Lotya M, Hernandez Y, King P J, et al. Liquid phase production of graphene by exfoliation of graphite in surfactant/water solutions. Journal of the American Chemical Society, 2009, 131(10): 3611-3620. DOI: 10.1021/ja807449u.
- [40]Coleman J N. Liquid-phase exfoliation of nanotubes and graphene. Advanced Functional Materials, 2009, 19(23): 3680-3695. DOI: 10.1002/adfm.200901640.
- [41]Cai M Z, Thorpe D, Adamson D H, et al. Methods of graphite exfoliation. Journal of Materials Chemistry, 2012, 22(48): 24992-25002. DOI: 10.1039/c2jm34517j.
- [42]Haar S, Bruna M, Lian J X, et al. Liquid-phase exfoliation of graphite into single- and few-layer graphene with alpha-functionalized alkanes. Journal of Physical Chemistry Letters, 2016, 7(14): 2714-2721. DOI: 10.1021/acs.jpclett.6b01260.
- [43]Coleman J N. Liquid exfoliation of defect-free graphene. Accounts of Chemical Research, 2012, 46(1): 14-22. DOI: 10.1021/ar300009f.
- [44]Paton K R, Varrla E, Backes C, et al. Scalable production of large quantities of defect-free few-layer graphene by shear exfoliation in liquids. Nature Materials, 2014, 13(6): 624-630. DOI: 10.1038/NMAT3944.
- [45]Tkalya E E, Ghislandi M, de With G, et al. The use of surfactants for dispersing carbon nanotubes and graphene to make conductive nanocomposites. Current Opinion in Colloid & Interface Science, 2012, 17(4): 225-231. DOI: 10.1016/j.cocis.2012.03.001.
- [46]Gai Y Z, Wang W C, Xiao D, et al. Ultrasound coupled with supercritical carbon dioxide for exfoliation of graphene: simulation and experiment. Ultrasonics Sonochemistry, 2018, 41: 181-188. DOI: 10.1016/j.ultsonch.2017.09.007.
- [47]Leydecker T, Eredia M, Liscio F, et al. Graphene exfoliation in the presence of semiconducting polymers for improved film homogeneity and electrical performances. Carbon, 2018, 130: 495-502. DOI: 10.1016/j.carbon.2018.01.042.
- [48]Kaur A, Singh R C. Managing the degree of exfoliation and number of graphene layers using probe sonication approach. Fullerenes Nanotubes and Carbon Nanostructures, 2017, 25(5): 318-326. DOI: 10.1080/1536383X.2017.1292254.

- [49] Pu N W, Wang C A, Sung Y, et al. Production of few-layer graphene by supercritical CO₂ exfoliation of graphite. *Materials Letters*, 2009, 63(23): 1987-1989. DOI: 10.1016/j.matlet.2009.06.031.
- [50] Wang W C, Wang Y, Gao Y H, et al. Control of number of graphene layers using ultrasound in supercritical CO₂ and their application in lithium-ion batteries. *Journal of Supercritical Fluids*, 2014, 85: 95-101. DOI: 10.1016/j.supflu.2013.11.005.
- [51] Wu B, Yang X N. A molecular simulation of interactions between graphene nanosheets and supercritical CO₂. *Journal of Colloid and Interface Science*, 2011, 361(1): 1-8. DOI: 10.1016/j.jcis.2011.05.021.
- [52] Li L, Xu J C, Li G H, et al. Preparation of graphene nanosheets by shear-assisted supercritical CO₂ exfoliation. *Chemical Engineering Journal*, 2016, 284(15): 78-84. DOI: 10.1016/j.cej.2015.08.077.
- [53] Kovtyukhova N I, Perea-Lopez N, Terrones M, et al. Atomically thin layers of graphene and hexagonal boron nitride made by solvent exfoliation of their phosphoric acid intercalation compounds. *ACS Nano*, 2017, 11(7): 6746-6754. DOI: 10.1021/acsnano.7b01311.
- [54] Kovtyukhova N I, Wang Y X, Berkdemir A, et al. Non-oxidative intercalation and exfoliation of graphite by Bronsted acids. *Nature Chemistry*, 2014, 6(11): 957-963. DOI: 10.1038/Nchem.2054.
- [55] Alanyalioglu M, Segura J J, Oro-Sole J, et al. The synthesis of graphene sheets with controlled thickness and order using surfactant-assisted electrochemical processes. *Carbon*, 2012, 50(1): 142-152. DOI: 10.1016/j.carbon.2011.07.064.
- [56] Yang S, Lohe M R, Müllen K, et al. New-generation graphene from electrochemical approaches: production and applications. *Advanced Materials*, 2016, 28(29): 6213-6221. DOI: 10.1002/adma.201505326.
- [57] Huang J Y, Qi L, Li J. In situ imaging of layer-by-layer sublimation of suspended graphene. *Nano Research*, 2010, 3(1): 43-50. DOI: 10.1007/s12274-010-1006-4.
- [58] Yang X C, Tang S J, Ding G Q, et al. Layer-by-layer thinning of graphene by plasma irradiation and post-annealing. *Nanotechnology*, 2012, 23(2): 025704. DOI: 10.1088/0957-4484/23/2/025704.
- [59] Hazra K S, Rafiee J, Rafiee M A, et al. Thinning of multilayer graphene to monolayer graphene in a plasma environment. *Nanotechnology*, 2011, 22(2): 025704. DOI: 10.1088/0957-4484/22/2/025704.
- [60] Han G H, Chae S J, Kim E S, et al. Laser thinning for monolayer graphene formation: heat sink and interference effect. *ACS Nano*, 2011, 5(1): 263-268. DOI: 10.1021/nn1026438.
- [61] Zhang L F, Feng S P, Xiao S Q, et al. Layer-controllable graphene by plasma thinning and post-annealing. *Applied Surface Science*, 2018, 441: 639-646. DOI: 10.1016/j.apsusc.2018.02.100.
- [62] Kiran G R, Chandu B, Acharyya S G, et al. One-step synthesis of bulk quantities of graphene from graphite by femtosecond laser ablation under ambient conditions. *Philosophical Magazine Letters*, 2017, 97(6): 229-234. DOI: 10.1080/09500839.2017.1320437.
- [63] Lin Z, Ye X H, Han J P, et al. Precise control of the number of layers of graphene by picosecond laser thinning. *Scientific Reports*, 2015, 5: 11662. DOI: 10.1038/Srep11662.
- [64] Dou W D, Yang Q D, Lee C S. The effects of oxygen on controlling the number of carbon layers in the chemical vapor deposition of graphene on a nickel substrate. *Nanotechnology*, 2013, 24(18): 185603. DOI: 10.1088/0957-4484/24/18/185603.
- [65] Baraton L, He Z B, Lee C S, et al. Synthesis of few-layered graphene by ion implantation of carbon in nickel thin films. *Nanotechnology*, 2011, 22(8): 085601. DOI: 10.1088/0957-4484/22/8/085601.
- [66] Sun J, Liu H M, Chen X, et al. Synthesis of graphene nanosheets with good control over the number of layers within the two-dimensional galleries of layered double hydroxides. *Chemical Communications*, 2012, 48(65): 8126-8128. DOI: 10.1039/c2cc33782g.
- [67] Muñoz R, Martínez L, López-Elvira E, et al. Direct synthesis of graphene on silicon oxide by low temperature plasma enhanced chemical vapor deposition. *Nanoscale*, 2018, 10(26): 12779-12787. DOI: 10.1039/C8NR03210F.
- [68] Hu Y F, Zhang Y M, Guo H, et al. Growth of thickness-controlled epitaxial graphene on on-axis 6H-SiC (C-face) substrate in graphite enclosure. *Journal of Materials Science: Materials in Electronics*, 2016, 27(6): 6242-6248. DOI: 10.1007/s10854-016-4555-9.
- [69] Aristov V Y, Chaika A N, Molodtsova O V, et al. Layer-by-layer graphene growth on β -SiC/Si (001). *ACS Nano*, 2018, 13(1): 526-535. DOI: 10.1021/acsnano.8b07237.
- [70] Narula U, Tan C M. Determining the parameters of importance of a graphene synthesis process using Design-of-Experiments method. *Applied Sciences-Basel*, 2016, 6(7): 204. DOI: 10.3390/App6070204.
- [71] Narula U, Tan C M, Lai C S. Growth mechanism for low temperature PVD graphene synthesis on copper using

- amorphous carbon. *Scientific Reports*, 2017, 7: 44112. DOI: 10.1038/srep44112.
- [72] Vijayaraghavan R K, Gaman C, Jose B, et al. Pulsed-plasma physical vapor deposition approach toward the facile synthesis of multilayer and monolayer graphene for anticoagulation applications. *ACS Applied Materials & Interfaces*, 2016, 8(7): 4878-4886. DOI: 10.1021/acsami.5b10952.
- [73] Lin L, Deng B, Sun J Y, et al. Bridging the gap between reality and ideal in chemical vapor deposition growth of graphene. *Chemical Reviews*, 2018, 118(18): 9281-9343. DOI: 10.1021/acs.chemrev.8b00325.
- [74] Li X S, Cai W W, Colombo L, et al. Evolution of graphene growth on Ni and Cu by carbon isotope labeling. *Nano Letters*, 2009, 9(12): 4268-4272. DOI: 10.1021/nl902515k.
- [75] Li X, Colombo L, Ruoff R S. Synthesis of graphene films on copper foils by chemical vapor deposition. *Advanced Materials*, 2016, 28(29): 6247-6252. DOI: 10.1002/adma.201504760.
- [76] Yang J, Hu P A, Yu G. Design of carbon sources: starting point for chemical vapor deposition of graphene. *2D Materials*, 2019, 6(4): 042003. DOI: 10.1088/2053-1583/Ab31bd.
- [77] Wassei J K, Mecklenburg M, Torres J A, et al. Chemical vapor deposition of graphene on copper from methane, ethane and propane: evidence for bilayer selectivity. *Small*, 2012, 8(9): 1415-1422. DOI: 10.1002/sml.201102276.
- [78] Sun H B, Xu J Q, Wang C L, et al. Synthesis of large-area monolayer and bilayer graphene using solid coronene by chemical vapor deposition. *Carbon*, 2016, 108: 356-362. DOI: 10.1016/j.carbon.2016.07.027.
- [79] Huet B, Raskin J-P. Role of Cu foil in-situ annealing in controlling the size and thickness of CVD graphene domains. *Carbon*, 2018, 129: 270-280. DOI: 10.1016/j.carbon.2017.12.043.
- [80] Rybin M G, Kondrashov I I, Pozharov A S, et al. In situ control of CVD synthesis of graphene film on nickel foil. *Physica Status Solidi B-Basic Solid State Physics*, 2018, 255(1): 1700414. DOI: 10.1002/pssb.201700414.
- [81] Gong Y P, Zhang X M, Liu G T, et al. Layer-controlled and wafer-scale synthesis of uniform and high-quality graphene films on a polycrystalline nickel catalyst. *Advanced Functional Materials*, 2012, 22(15): 3153-3159. DOI: 10.1002/adfm.201200388.
- [82] Kayhan E, Prasad R M, Gurlo A, et al. Synthesis, characterization, electronic and gas-sensing properties towards H₂ and CO of transparent, large-area, low-layer graphene. *Chemistry-A European Journal*, 2012, 18(47): 14996-15003. DOI: 10.1002/chem.201201880.
- [83] Kairi M I, Khavarian M, Bakar S A, et al. Recent trends in graphene materials synthesized by CVD with various carbon precursors. *Journal of Materials Science*, 2018, 53(2): 851-879. DOI: 10.1007/s10853-017-1694-1.
- [84] Scaparro A M, Miseikis V, Coletti C, et al. Investigating the CVD synthesis of graphene on Ge(100): toward layer-by-layer growth. *ACS Applied Materials & Interfaces*, 2016, 8(48): 33083-33090. DOI: 10.1021/acsami.6b11701.
- [85] Wu Y P, Chou H, Ji H X, et al. Growth mechanism and controlled synthesis of AB-stacked bilayer graphene on Cu-Ni alloy foils. *ACS Nano*, 2012, 6(9): 7731-7738. DOI: 10.1021/nn301689m.
- [86] Lee J S, Jang C W, Kim J M, et al. Graphene synthesis by C implantation into Cu foils. *Carbon*, 2014, 66: 267-271. DOI: 10.1016/j.carbon.2013.08.066.
- [87] Kato R, Minami S, Koga Y, et al. High growth rate chemical vapor deposition of graphene under low pressure by RF plasma assistance. *Carbon*, 2016, 96: 1008-1013. DOI: 10.1016/j.carbon.2015.10.061.
- [88] Naghdi S, Rhee K Y, Park S J. A catalytic, catalyst-free, and roll-to-roll production of graphene via chemical vapor deposition: low temperature growth. *Carbon*, 2018, 127: 1-12. DOI: 10.1016/j.carbon.2017.10.065.
- [89] Li M L, Liu D H, Wei D C, et al. Controllable synthesis of graphene by plasma-enhanced chemical vapor deposition and its related applications. *Advanced Science*, 2016, 3(11): 1600003. DOI: 10.1002/Adv.201600003.
- [90] Chaika A N, Aristov V Y, Molodtsova O V. Graphene on cubic-SiC. *Progress in Materials Science*, 2017, 89: 1-30. DOI: 10.1016/j.pmatsci.2017.04.010.
- [91] Norimatsu W, Kusunoki M. Epitaxial graphene on SiC{0001}: advances and perspectives. *Physical Chemistry Chemical Physics*, 2014, 16(8): 3501-3511. DOI: 10.1039/c3cp54523g.
- [92] Yazdi G R, Iakimov T, Yakimova R. Epitaxial graphene on SiC: a review of growth and characterization. *Crystals*, 2016, 6(5): 53. DOI: 10.3390/Cryst6050053.
- [93] Nyakiti L O, Myers-Ward R L, Wheeler V D, et al. Bilayer graphene grown on 4H-SiC (0001) step-free mesas. *Nano Letters*, 2012, 12(4): 1749-1756. DOI: 10.1021/nl203353f.
- [94] Kumar B, Baraket M, Paillet M, et al. Growth protocols and characterization of epitaxial graphene on SiC elaborated in a graphite enclosure. *Physica E-Low-Dimensional Systems & Nanostructures*, 2016, 75: 7-14. DOI: 10.1016/j.physe.2015.07.022.
- [95] de Heer W A, Berger C, Wu X S, et al. Epitaxial graphene.

- Solid State Communications, 2007, 143(1-2): 92-100. DOI: 10.1016/j.ssc.2007.04.023.
- [96] Gupta B, Notarianni M, Mishra N, et al. Evolution of epitaxial graphene layers on 3C SiC/Si (111) as a function of annealing temperature in UHV. Carbon, 2014, 68: 563-572. DOI: 10.1016/j.carbon.2013.11.035.
- [97] Zhang H, Ding F Z, Li H, et al. Controlled synthesis of monolayer graphene with a high quality by pyrolysis of silicon carbide. Materials Letters, 2019, 244: 171-174. DOI: 10.1016/j.matlet.2019.02.038.
- [98] Riedl C, Zakharov A A, Starke U. Precise in situ thickness analysis of epitaxial graphene layers on SiC(0001) using low-energy electron diffraction and angle resolved ultraviolet photoelectron spectroscopy. Applied Physics Letters, 2008, 93(3): 033106. DOI: 10.1063/1.2960341.
- [99] Pandey P A, Bell G R, Rourke J P, et al. Physical vapor deposition of metal nanoparticles on chemically modified graphene: observations on metal-graphene interactions. Small, 2011, 7(22): 3202-3210. DOI: 10.1002/sml.201101430.
- [100] Banerjee A N, Min B K, Joo S W. Synthesis of metal-incorporated graphitic microporous carbon terminated with highly-ordered graphene walls-Controlling the number of graphene layers by ambient-temperature metal sputtering. Applied Surface Science, 2013, 268: 588-600. DOI: 10.1016/j.apsusc.2013.01.040.
- [101] Garlow J A, Barrett L K, Wu L J, et al. Large-area growth of turbostratic graphene on Ni(111) via physical vapor deposition. Scientific Reports, 2016, 6: 19804. DOI: 10.1038/Srep19804.
- [102] Narula U, Tan C M. Engineering a PVD-based graphene synthesis method. IEEE Transactions on Nanotechnology, 2017, 16(5): 784-789. DOI: 10.1109/TNANO.2017.2670604.
- [103] Narula U, Tan C M, Lai C S. Copper induced synthesis of graphene using amorphous carbon. Microelectronics Reliability, 2016, 61: 87-90. DOI: 10.1016/j.microrel.2016.01.005.
- [104] Quesnel E, Roux F, Emieux F, et al. Graphene-based technologies for energy applications, challenges and perspectives. 2D Materials, 2015, 2(3): 030204. DOI: 10.1088/2053-1583/2/3/030204.
- [105] Palaniselvam T, Baek J-B. Graphene based 2D-materials for supercapacitors. 2D Materials, 2015, 2(3): 032002. DOI: 10.1088/2053-1583/2/3/032002.
- [106] Kuilla T, Bhadra S, Yao D H, et al. Recent advances in graphene based polymer composites. Progress in Polymer Science, 2010, 35(11): 1350-1375. DOI: 10.1016/j.progpolymsci.2010.07.005.
- [107] Phiri J, Gane P, Maloney T C. General overview of graphene: production, properties and application in polymer composites. Materials Science and Engineering B: Advanced Functional Solid-State Materials, 2017, 215: 9-28. DOI: 10.1016/j.mseb.2016.10.004.
- [108] Abbasi E, Akbarzadeh A, Kouhi M, et al. Graphene: synthesis, bio-applications, and properties. Artificial Cells Nanomedicine & Biotechnology, 2014, 44(1): 150-156. DOI: 10.3109/21691401.2014.927880.
- [109] Shareena T P D, McShan D, Dasmahapatra A K, et al. A review on graphene-based nanomaterials in biomedical applications and risks in environment and health. Nano-Micro Letters, 2018, 10(3): 53. DOI: 10.1007/s40820-018-0206-4.
- [110] Liu M M, Zhang R Z, Chen W. Graphene-supported nanoelectrocatalysts for fuel cells: synthesis, properties, and applications. Chemical Reviews, 2014, 114(10): 5117-5160. DOI: 10.1021/cr400523y.
- [111] Sun Y, Zhang J W, Zong Y, et al. Crystalline-amorphous permalloy@iron oxide core-shell nanoparticles decorated on graphene as high-efficiency, lightweight, and hydrophobic microwave absorbents. ACS Applied Materials & Interfaces, 2019, 11(6): 6374-6383. DOI: 10.1021/acsami.8b18875.
- [112] Ma Z L, Wei A J, Ma J Z, et al. Lightweight, compressible and electrically conductive polyurethane sponges coated with synergistic multiwalled carbon nanotubes and graphene for piezoresistive sensors. Nanoscale, 2018, 10(15): 7116-7126. DOI: 10.1039/c8nr00004b.
- [113] Wang F, Wu Y D, Huang Y D. Novel application of graphene oxide to improve hydrophilicity and mechanical strength of aramid nanofiber hybrid membrane. Composites Part A: Applied Science and Manufacturing, 2018, 110: 126-132. DOI: 10.1016/j.compositesa.2018.04.023.
- [114] Oh J-H, Kim J, Lee H, et al. Directionally antagonistic graphene oxide-polyurethane hybrid aerogel as a sound absorber. ACS Applied Materials & Interfaces, 2018, 10(26): 22650-22660. DOI: 10.1021/acsami.8b06361.
- [115] Choi W, Lahiri I, Seelaboyina R, et al. Synthesis of graphene and its applications: a review. Critical Reviews in Solid State and Materials Sciences, 2010, 35(1): 52-71. DOI: 10.1080/10408430903505036.
- [116] Maharubin S, Zhang X, Zhu F L, et al. Synthesis and applications of semiconducting graphene. Journal of Nanomaterials, 2016, 2016: 1-19. DOI: 10.1155/2016/6375962.
- [117] El-Kady M F, Shao Y L, Kaner R B. Graphene for batteries, supercapacitors and beyond. Nature Reviews Materials, 2016,

1: 1-14. DOI: 10.1038/Natrevmats.2016.33.

- [118] Nag A, Mitra A, Mukhopadhyay S C. Graphene and its sensor-based applications: a review. *Sensors and Actuators A: Physical*, 2018, 270: 177-194. DOI: 10.1016/j.sna.2017.12.028.
- [119] Rowley-Neale S J, Randviir E P, Dena A S A, et al. An overview of recent applications of reduced graphene oxide as a basis of electroanalytical sensing platforms. *Applied Materials Today*, 2018, 10: 218-226. DOI: 10.1016/j.apmt.2017.11.010.
- [120] Loh K P, Bao Q L, Eda G, et al. Graphene oxide as a chemically tunable platform for optical applications. *Nature Chemistry*, 2010, 2(12): 1015-1024. DOI: 10.1038/Nchem.907.
- [121] Liu G P, Jin W Q, Xu N P. Graphene-based membranes. *Chemical Society Reviews*, 2015, 44(15): 5016-5030. DOI: 10.1039/c4cs00423j.
- [122] Huang L, Zhang M, Li C, et al. Graphene-based membranes for molecular separation. *Journal of Physical Chemistry Letters*, 2015, 6(14): 2806-2815. DOI: 10.1021/acs.jpclett.5b00914.
- [123] Lin X H, Gai J G. Synthesis and applications of large-area single-layer graphene. *RSC Advances*, 2016, 6(22): 17818-17844. DOI: 10.1039/c5ra27349h.
- [124] Xu J, Cao Z, Zhang Y L, et al. A review of functionalized carbon nanotubes and graphene for heavy metal adsorption from water: preparation, application, and mechanism. *Chemosphere*, 2018, 195: 351-364. DOI: 10.1016/j.chemosphere.2017.12.061.
- [125] Wassei J K, Kaner R B. Graphene, a promising transparent conductor. *Materials Today*, 2010, 13(3): 52-59. DOI: 10.1016/S1369-7021(10)70034-1.
- [126] Sun Z Z, Raji A-R O, Zhu Y, et al. Large-area Bernal-stacked bi-, tri-, and tetralayer graphene. *ACS Nano*, 2012, 6(11): 9790-9796. DOI: 10.1021/nn303328e.
- [127] Ferrari A C, Bonaccorso F, Fal'Ko V, et al. Science and technology roadmap for graphene, related two-dimensional crystals, and hybrid systems. *Nanoscale*, 2015, 7(11): 4598-4810. DOI: 10.1039/C4NR01600A.
- [128] Banerjee S K, Register L F, Tutuc E, et al. Graphene for CMOS and beyond CMOS applications. *Proceedings of the IEEE*, 2010, 98(12): 2032-2046. DOI: 10.1109/Jproc.2010.2064151.
- [129] Yan H G. Bilayer graphene: physics and application outlook in photonics. *Nanophotonics*, 2015, 4(2): 115-127. DOI: 10.1515/nanoph-2014-0019.
- [130] Fang W J, Hsu A L, Song Y, et al. A review of large-area bilayer graphene synthesis by chemical vapor deposition. *Nanoscale*, 2015, 7(48): 20335-20351. DOI: 10.1039/C5NR04756K.
- [131] Wessely P J, Schwalke U. In situ CCVD grown bilayer graphene transistors for applications in nanoelectronics. *Applied Surface Science*, 2014, 291: 83-86. DOI: 10.1016/j.apsusc.2013.09.142.
- [132] Gong L, Young R J, Kinloch I A, et al. Optimizing the reinforcement of polymer-based nanocomposites by graphene. *ACS Nano*, 2012, 6(3): 2086-2095. DOI: 10.1021/nn203917d.
- [133] Graf D, Molitor F, Ensslin K, et al. Spatially resolved Raman spectroscopy of single- and few-layer graphene. *Nano Letters*, 2007, 7(2): 238-242. DOI: 10.1021/nl061702a.
- [134] Li Y F, Yang W, Tu Z Q, et al. Schottky junction solar cells based on graphene with different numbers of layers. *Applied Physics Letters*, 2014, 104(4): 043903. DOI: 10.1063/1.4863683.
- [135] Martin-Olmos C, Rasool H I, Weiller B H, et al. Graphene MEMS: AFM probe performance improvement. *ACS Nano*, 2013, 7(5): 4164-4170. DOI: 10.1021/nn400557b.
- [136] Zang X, Zhou Q, Chang J, et al. Graphene and carbon nanotube (CNT) in MEMS/NEMS applications. *Microelectronic Engineering*, 2015, 132: 192-206. DOI: 10.1016/j.mee.2014.10.023.
- [137] Wang Q G, Hong W, Dong L. Graphene "microdrums" on a freestanding perforated thin membrane for high sensitivity MEMS pressure sensors. *Nanoscale*, 2016, 8(14): 7663-7671. DOI: 10.1039/C5NR09274D.
- [138] Khan Z H, Kermany A R, Ochsner A, et al. Mechanical and electromechanical properties of graphene and their potential application in MEMS. *Journal of Physics D: Applied Physics*, 2017, 50(5): 053003. DOI: 10.1088/1361-6463/50/5/053003.
- [139] Lee C, Li Q Y, Kalb W, et al. Frictional characteristics of atomically thin sheets. *Science*, 2010, 328(5974): 76-80. DOI: 10.1126/science.1184167.
- [140] Pu J B, Mo Y F, Wan S H, et al. Fabrication of novel graphene-fullerene hybrid lubricating films based on self-assembly for MEMS applications. *Chemical Communications*, 2014, 50(4): 469-471. DOI: 10.1039/C3CC47486K.
- [141] Liu H, Yang S M, Wang J H, et al. Multilayer graphene sheets assembled by Langmuir-Blodgett for tribology application. 2012 12th IEEE International Conference on Nanotechnology (IEEE-NANO). Piscataway: IEEE, 2012. 1-5. DOI: 10.1109/NANO.2012.6321997.
- [142] Zhou M, Bi H, Lin T Q, et al. Heat transport enhancement of thermal energy storage material using graphene/ceramic

composites. Carbon, 2014, 75: 314-321. DOI: 10.1016/j.carbon.2014.04.009.

- [143] Liang J Z. Impact fracture behavior and morphology of polypropylene/graphene nanoplatelets composites. Polymer Composites, 2019, 40(S1): E511-E516. DOI: 10.1002/pc.24826.
- [144] Luo N Q, Huang Y, Liu J, et al. Hollow-structured graphene-silicone-composite-based piezoresistive sensors: decoupled property tuning and bending reliability. Advanced Materials, 2017, 29(40): 1702675. DOI: 10.1002/adma.201702675.
- [145] Li X G, Feng H, Huang M R, et al. Ultrasensitive Pb(II) potentiometric sensor based on copolyaniline nanoparticles in a plasticizer-free membrane with a long lifetime. Analytical Chemistry, 2012, 84(1): 134-140. DOI: 10.1021/ac2028886.
- [146] Huang M R, Ding Y B, Li X G, et al. Synthesis of semiconducting polymer microparticles as solid ionophore with abundant complexing sites for long-life Pb(II) sensors. ACS Applied Materials & Interfaces, 2014, 6(24): 22096-22107. DOI: 10.1021/am505463f.
- [147] Huang M R, Ding Y B, Li X G. Lead-ion potentiometric sensor based on electrically conducting microparticles of sulfonic phenylenediamine copolymer. Analyst, 2013, 138(13): 3820-3829. DOI: 10.1039/c3an00346a.
- [148] Huang M R, Ding Y B, Li X G. Combinatorial screening of potentiometric Pb(II) sensors from polysulfoaminoanthraquinone solid ionophore. ACS Combinatorial Science, 2014, 16(3): 128-138. DOI: 10.1021/co400140g.
- [149] Huang M R, Rao X W, Li X G, et al. Lead ion-selective electrodes based on polyphenylenediamine as unique solid ionophores. Talanta, 2011, 85(3): 1575-1584. DOI: 10.1016/j.talanta.2011.06.049.
- [150] Li X G, Ma X L, Huang M R. Lead(II) ion-selective electrode based on polyaminoanthraquinone particles with intrinsic conductivity. Talanta, 2009, 78(2): 498-505. DOI: 10.1016/j.talanta.2008.11.045.